Redox Biology 85 (2025) 103760

Contents lists available at ScienceDirect

Redox Biology

journal homepage: www.elsevier.com/locate/redox

Obesity-induced arterial redox imbalance involving mitochondrial NOX4, endothelial dysfunction, and ER stress underlie kidney injury compensated by enhanced mitochondrial bioenergetics

Cristina Contreras [a,*], Mercedes Muñoz [a,1], Óscar Freire-Agulleiro [c,1], Ánxela Estévez [c,1], María Pilar Martínez [b], Lucia Olmos [a], Alfonso Gómez del Val [a], Claudia Rodríguez [a], Ramona A. Silvestre [e], Ana Sánchez [a], Sara Benedito [a], Luis Rivera [a], Javier Sáenz-Medina [d], Miguel López [c], María Elvira López-Oliva [a], Dolores Prieto [a,**]

[a] Departamento de Fisiología, Facultad de Farmacia, Universidad Complutense, Madrid, Spain
[b] Departamento de Histología y Embriología, Universidad Complutense, Madrid, Spain
[c] Departmento de Fisiología, Universidad de Santiago de Compostela, Spain
[d] Departamento de Urología, Hospital Universitario Ramón y Cajal3, Madrid, Spain
[e] Biochemistry Service, Hospital Universitario Puerta de Hierro, Majadahonda, Spain

ARTICLE INFO

Keywords:
Obesity
Kidney injury
Vascular mitochondria
NOX4
Redox imbalance
Endothelial dysfunction
ER stress

ABSTRACT

Mitochondrial reactive oxygen species (mtROS) are key pathogenic factors in the microvascular complications of metabolic disorders including nephropathy. However, the effects of obesity on kidney vascular mitochondria and endothelial function remain unclear. We assessed here the specific impact of obesity on endothelial function, mtROS-derived oxidative stress and mitochondrial bioenergetics of kidney preglomerular arteries in rat models of high fat diet (HFD)-induced obesity and endoplasmic reticulum (ER) stress. Arterial function was assessed in microvascular myographs, mitoSOX and Amplex Red fluorimetry were used to measure mtROS levels, and mitochondrial respiration was evaluated in renal preglomerular arteries by using an Agilent Seahorse XF Pro analyzer. Expression of mitochondria regulators and endoplasmic reticulum (ER) stress markers was analyzed by Western blot. We demonstrate here that HFD induces kidney injury and structural alterations including glomerulomegalia and fibrosis associated to redox imbalance with augmented mitochondrial superoxide, endothelial dysfunction, and endoplasmic reticulum (ER) stress in renal preglomerular arteries. Both HFD and ER stress lead to impaired biogenesis and down-regulation of the peroxisome proliferator-activated receptor γ coactivator 1α (PGC-1α) and NADPH oxidase 4 (NOX4), and lower levels of H_2O_2 that contribute to endothelial dysfunction. These changes are in turn associated with enhanced arterial mitochondrial respiration along with up-regulation of mitochondrial cytochrome *c* oxidase subunit 4 COX-IV likely related to hemodynamic changes in kidney preglomerular arteries leading to increased glomerular hyperfiltration rate (GFR) to supply function of injured glomeruli. The present findings therefore link adaptative changes in mitochondrial bioenergetics to obesity-induced impaired redox balance, endothelial dysfunction and ER stress in preglomerular arteries underlying kidney injury.

1. Introduction

Obesity is a public health problem whose increasing prevalence worldwide reaches pandemic proportions, impacting children and adolescents and significantly contributing to the onset of diabetes and cardiovascular disease (CVD) [1,2]. Considered as a major cardiovascular risk factor, obesity is frequently linked to various metabolic and vascular abnormalities such as visceral adiposity, dyslipidemia, insulin resistance, and hypertension, all of which promote the development of chronic kidney disease (CKD) [3]. However, obesity itself is a risk factor for the development of CKD independent of other comorbidities such as

* Corresponding author. Departamento de Fisiología Facultad de Farmacia Universidad Complutense de Madrid 28040, Madrid, Spain.
** Corresponding author. Departamento de Fisiología Facultad de Farmacia Universidad Complutense de Madrid, 28040, Madrid Spain.
E-mail addresses: criscont@ucm.es (C. Contreras), dprieto@ucm.es (D. Prieto).
[1] equally contributed.

https://doi.org/10.1016/j.redox.2025.103760
Received 16 June 2025; Received in revised form 4 July 2025; Accepted 7 July 2025
Available online 12 July 2025

Abbreviations

ACh	acetylcholine
ATF6	activating transcription factor 6
BiP	binding immunoglobulin protein
CHOP C/EBP	Homologous Protein
CKD	chronic kidney disease
COX-IV	cytochrome c oxidase subunit 4
CRC	concentration-response curve
CVD	cardiovascular disease
ECAR	extracelular acidification rate
eNOS	endothelial nitric oxide
ER	endoplasmic reticulum
FCCP	carbonyl cyanide 4-(trifluoromethoxy) phenylhydrazone
HFD	high fat diet
H_2O_2	hydrogen peroxide
KPSS	high-K^+ physiological saline solution
L-NOARG	L-NG-nitro-arginine
MnSOD	manganese superoxide dismutase
mtROS	mitochondrial reactive oxygen species
NO	nitric oxide
NOS	nitric oxide synthase
NOX1	NADPH oxidase 1
NOX4	NADPH oxidase 4
OCR	oxygen consumption rate
OXPHOS	oxidative phosphorylation
$O_2^{\bullet-}$	superoxide anion
peIF2α	phosphorylated eukaryotic translation initiation factor 2A
PERK	protein kinase R-like endoplasmic reticulum kinase
pIRE1α	phosphorylated inositol-requiring enzyme-1 alpha
Phe	phenylephrine
PSS	physiological saline solution
PVDF	polyvinylidene fluoride
RFU	relative fluorescence units
ROS	reactive oxygen species
SDS-PAGE	polyacrylamide gel
STD	standard diet
UPR	unfolded protein response

diabetes or hypertension [4–6], and is associated with increased risk of end-stage renal disease [5,7]. Obesity-induced kidney injury manifests as glomerular hypertrophy, tubular injury and interstitial fibrosis leading to progressive loss of renal function, abnormal renal hemodynamics, dysfunction of endothelial cells and podocytes and microalbuminuria [6–10]. Mitochondria are cytoplasmic organelles that supply 90 % of cell energy during mitochondrial respiration by generating ATP via oxidative phosphorylation (OXPHOS) through the electron transport chain (ETC). Since this process is reliant on oxygen consumption, mitochondria represent the primary intracellular source of reactive oxygen species (ROS) [11]. The kidney is an organ with high energy consumption and mitochondrial fatty acid β-oxidation is the main source of ATP, and hence mitochondrial dysfunction plays a critical role in the pathogenesis of renal disease [12]. Mitochondrial injury has also been involved as a major contributing factor for several chronic noninfectious, nontransmissible diseases often associated with low-grade inflammation such as CVD, cancer, obesity, and type 2 diabetes, diseases having the ability to either damage mitochondria or interfere with mitochondrial repair [13,14]. Dysfunctional mitochondria limit energy production by impairing mitochondrial biogenesis and OXPHOS, increasing ROS generation and inducing apoptosis, events that exacerbate mitochondrial damage resulting in tissue damage and dysfunction [11,14].

Oxidative stress is considered the trigger of renal inflammation in metabolic disease-associated nephropathy. NADPH oxidases (NOX) and mitochondria are the main sources of ROS in the kidney [9,15]. Increased ROS production in mesangial, endothelial and tubular cells mostly derived from mitochondrial NOX4 has been found associated with both diabetes- [16–18] and obesity-related kidney disease [8,19]. Excess of mitochondrial ROS (mtROS) was initially accepted as a major cause of diabetic complications [20], including nephropathy. However, both reduced superoxide generation and mitochondrial biogenesis [21,22], and mtROS overproduction linked to inflammation and tubular oxidative injury [15] have been reported in diabetic nephropathy. Information about kidney mitochondrial function in obesity is limited and controversial. Thus, oxidative stress derived from mitochondria was linked to kidney inflammation and structural alterations but preserved respiratory function and biogenesis in response to lipid overload in high fat diet (HFD)-fed mice [23]. In contrast, no major inflammatory or structural changes but renal dysfunction associated to decreased ATP levels indicative of impaired OXPHOS were found in the kidney of genetic mouse models of obesity [24].

Mitochondrial dysfunction affects other cell organelles such as the endoplasmic reticulum (ER), involved in several key functions including synthesis, maturation, folding, and transportation of proteins, as well as lipid biosynthesis and calcium homeostasis. Disruptions in ER homeostasis, as observed in stress conditions such as ischemia, glucose deprivation, calcium overload, and oxidative stress, can result in the ER losing its ability to process proteins leading to the accumulation of unfolded proteins. This triggers an adaptive response known as the unfolded protein response (UPR) aimed at solving the stress situation, phenomenon referred as ER stress response [25]. ER stress and initiation of the UPR pathways significantly contribute to degenerative diseases, diabetes, obesity, atherosclerosis, cancer, and various inflammatory processes [26,27]. In the kidney, ER stress poses a significant threat to renal function, and has been associated with renal pathologies such as nephrotic syndrome, segmental glomerulosclerosis [28,29], and diabetic nephropathy [30] which contribute to both glomerular and tubulointerstitial injury, thereby promoting the onset and progression of kidney disease. On the other hand, growing evidence supports a direct connection between ER stress and changes in metabolism and endothelial dysfunction [31–33].

Recent studies have demonstrated that protection of mitochondria prevents renal inflammation, glomerulopathy and renal injury in obesity which suggests that mitochondrial dysfunction is involved in obesity-associated nephropathy [34]. Obesity and metabolic syndrome also impact vascular mitochondrial function by increasing oxidative stress and impairing endothelial function and mitochondrial bioenergetics [33,35–37]. While information on the effects of obesity on kidney mitochondrial function is limited and controversial showing either impaired mitochondrial respiration, ER stress and renal dysfunction [24] or preserved bioenergetics along with augmented mtROS levels [23], little is known on the selective impact of obesity on kidney vascular mitochondria. Therefore, we used a rat model of diet-induced obesity to dissect the impact of obesity on endothelial function, oxidative stress, and mitochondrial bioenergetics of kidney preglomerular arteries. We hypothesized that obesity and metabolic syndrome may impair mitochondrial function of the renal vasculature leading to ER stress and endothelial and vascular dysfunction, which in turn may contribute to obesity-associated kidney injury.

2. Materials and methods

2.1. Animal model

Age-matched male Wistar rats purchased from *Janvier Labs (Spain)* at

3-weeks-old were housed at the Pharmacy School animal care facility with artificial 12 h light/dark cycles (8:00–20:00h), under controlled humidity and temperature conditions. Animals had free access to water and were fed *ad libitum* for 15 weeks starting after weaning with high fat diet (HFD; with 60 kcal% fat, D12492 Research *Diets*, *USA*) or standard diet (STD; with 3,5 kcal % fat, *Rod14H LASQCdiet®, Germany*), to generate diet-induced obesity and their controls, respectively. After 15 more weeks, animals were euthanized and kidneys were quickly removed and placed in cold physiological saline solution (PSS; *NaCl* 119 mM, $NaHCO_3$ 25 mM, *glucose* 11 mM, *KCl 4*.7 mM, $CaCl_2$ *1*.5 mM, $MgSO_4$ *1*.18 mM, KH_2PO_4 *1*.17 mM *and EDTA 0*.027 mM). Animal care and experimental protocols complied with the European Union Guidelines for the Care and Protection of Animals Used for Scientific Purposes (*European Union Directive 2010/63/EU*) and were approved by Universidad Complutense and Comunidad de Madrid Institutional Animal Care and Use Comittees (Project ID Ref PROEX 192.3/20). Blood quantitative determination of glucose, triglycerides, and lactate were measured in a drop of blood obtained from a little incision in the rat tail with Accutrend® Plus meter using test strips specific for each of these blood parameters *(Roche Diagnostics, Germany)*.

A rat model of chemically-induced ER stress was established by intraperitoneal injection of 0.30 mg/kg tunicamycin *(bioWORLD, USA)* to 16 weeks-old male Wistar every second day for 2 weeks.

2.2. Kidney function and histopathological morphometric analysis

Urine samples were collected over a 24 h period by placing the animals in metabolic cages. Urine output was measured, and Combur Tests was used for *in vitro* semi quantitative determination of pH and proteins. Estimated glomerular filtration rate was also calculated by measuring cystatin C (CYS) levels in serum by a particle-enhanced nephelometric immunoassay *(BNII, Siemens Healthcare Diagnostics)* [38,39]. For the morphometric analysis, kidneys from STD and HFD rats were fixed overnight in 4 % paraformaldehyde dissolved in 0.1 M phosphate buffer pH 7.4, and then embedded in paraffin. Serial sections (4 μm) were mounted on glass slides, hydrated, and stained with hematoxylin and eosin. To assess histopathological changes, 10 images of stained sections were acquired under a light microscope using a Leica DM LB2 microscope and a Leica DFC 320 digital camera *(Leica, Spain)*. Morphometric analysis was performed wby using ImageJ 1.5.4 software *(U. S. National Institutes of Health, Bethesda, MD, USA)*. All slides were independently examined by two different researchers under blinded conditions. In the kidney, the number of glomeruli, glomerular area (GA), Bowman's space and number of cells per glomeruli were evaluated. Measurements were taken from the average of 5 cortical fields, or 10 glomeruli cut at the vascular pole for each kidney. Glomerular volume (GV) was calculated using the formula for quantification of renal pathology $GV = 1.2545\ (GA)^{1,5}$ [40].

2.3. Masson's trichrome staining analysis

Digital images of renal tissue sections stained with Masson's trichrome were analyzed to assess collagen deposition. Regions of interest (ROIs) were defined to include the entire glomerular tuft in each image. Image analysis was conducted using Fiji (ImageJ v.1.54), employing the Color Deconvolution plugin with the Masson Trichrome vector to isolate the blue-stained collagen channel. A consistent threshold was applied to quantify collagen content as a percentage of the total glomerular area. For each kidney, data were expressed as the mean of 10 cortical fields or 10 glomeruli sectioned at the vascular pole.

2.4. Dissection and mounting of arteries

Renal interlobar arteries, 2nd-3rd order branches of the major renal artery (Fig. S1), were isolated from the kidney of HFD and STD rats, and carefully dissected by removing the surrounding connective and fatty tissue. Small samples of both renal arteries and cortex (at the intersection of renal cortex and medulla) were also dissected out for measurement of mitochondrial ROS and H_2O_2 [9,41]. Arterial segments were mounted in microvascular myographs (*Danish Myotechnology, Denmark*) and stabilized for 30 min in PSS at 37 °C bubbled with 95 % O_2/5 % CO_2. The relationship between passive wall tension and internal circumference was calculated for each artery, and from this the internal circumference corresponding to a transmural pressure of 100 mmHg for a relaxed vessel in situ, $L_{100,}$ was determined. Arteries were set to an internal circumference L_1 equal to 90 % $L_{100,}$ at which force development is maximal.

2.5. Experimental procedure for the functional experiments

At the beginning of each experiment, vessel viability was tested by stimulating the arteries twice with a high K^+ solution (KPSS, equivalent to PSS except that NaCl was exchanged for KCl on an equimolar basis giving a final 124 mM K^+ concentration). Semilogarithmic cumulative concentration-responses curves (CRC) to the α_1-adrenergic agonist phenylephrine (Phe, 0.01–30 μM) were performed to evaluate vasoconstrictor responses of renal arteries. Furthermore, CRC to acetylcholine (ACh, 0.01–30 μM) were constructed to evaluate endothelial function in arteries precontracted with Phe (0.1–0.5 μM). To assess the involvement of ROS from mitochondria or ROS derived from NOX in preglomerular intrarenal arteries from HFD or tunicamycin-treated rats and their respective controls (STD or vehicle-treated rats), CCR for ACh were performed in the absence and presence of the eNOS inhibitor NG-nitro-L-arginine (L-NOARG, 100 μM), the mitochondrial ROS scavenger mitoTempo (0.1 μM), the non-selective NOX inhibitor apocynin (10 μM) or the selective NOX1 inhibitor NoxA1ds (0.3 μM) *(Merk-Sigma Aldrich, Spain)*. Endothelium-independent relaxations were assessed in CCR to the NO donor S-nitroso-N-acetylpenicillamine, SNAP (10^{-8} -10^{-5}) in Phe-precontracted renal preglomerular arteries.

2.6. Measurement of H_2O_2 by Amplex Red

Hydrogen peroxide (H_2O_2) generation was measured by Amplex Red assay Kit (Thermo Fisher Scientific, Life Technologies SA, Spain) in renal arteries and cortex from HFD and STD rats [9,42]. Samples were equilibrated in HEPES-PSS for 30 min at room temperature and then transferred to microtiter plate black wells with 100 μM Amplex Red solution and horseradish peroxidase (10 U/ml) diluted at reaction buffer 37 °C. Fluorescence derived from interaction between H_2O_2 and Amplex Red (reaction 1:1) was measured in a fluorimeter (*BMG Fluostar Optima*) with excitation filter of 544 nm and emission filter of 590 nm). Background fluorescence was subtracted from the counting values, being referred to H_2O_2 production that was normalized to dry sample weight.

2.7. Measurement of mitochondrial ROS by MitoSOX

Mitochondrial superoxide ($O_2^{\cdot-}$) (mtROS) were measured in segments of renal arteries and cortex samples from STD and HFD rats by using the mitochondria-targeted derivative of hydroethidine MioSOX (*Molecular Probes, Fisher Scientific, Spain*) [67]. Samples were equilibrated in HEPES-physiological saline solution at room temperature and then incubated with 15 μM MitoSOX for 30 min at 37 °C. Fluorescence was measured in a fluorimeter (*BMG Fluostar Optima*, emission filter of 510 nm and excitation filter of 580 nm). Background fluorescence was subtracted from the counting values, and mtROS production was normalized to dry sample weight.

2.8. Measurement of superoxide production by chemiluminescence

Basal and NADPH-stimulated $O_2^{\cdot-}$ levels of were detected by lucigenin enhanced chemiluminescence, as previously described [42]. Renal cortex and interlobar arteries samples from control and

tunicamycin-induced ER stress rats were maintained in PSS for 30 min at room temperature for equilibration, and then incubated in the absence (controls) and presence of the extracellular NADPH (100 μM) alone or after treatment with the NOX inhibitor apocynin to determine basal and Nox-derived $O_2^{\cdot-}$ levels. Samples were thereafter transferred to microtiter plate wells containing 5 μM bis-N-methylacridinium nitrate (lucigenin). Chemiluminescence was measured in a luminometer (*BMG Fluostar Optima*), and for calculation baseline values were subtracted from the counting values under the different experimental conditions and superoxide production was normalized to dry tissue weight.

2.9. Mitochondrial respiration measurements

Mitochondrial bioenergetics were assessed in intact fresh kidney preglomerular arteries by Agilent Seahorse XF HS Mini analyzer to perform real-time measurements of mitochondrial oxygen consumption rate (OCR), as measurement of respiration, and extracellular acidification rate (ECAR), as an indicator of glycolysis, with a Mitostress Assay. Segments about 2 mm long of freshly isolated renal preglomerular arteries were placed in the bottom of wells of the XF HS islet capture microplate, as previously described for small arteries [43,44]. The oxygen and proton concentrations in the medium were then repeatedly measured by oxygen and hydrogen ion-selective fluorophores of the Seahorse XF HS analyzer to calculate OCR (pmol/O_2/min) and ECAR (milipH/min). Each well was filled with 200 μl of XF assay medium containing 5.0 mM glucose, 2 mM pyruvate and 2 mM glutamine, and maintained at 37 °C for 20 min in a non-CO_2 incubator before measurement O_2 and H^+ levels under basal conditions, and after adding oligomycin (50 μM, blocking the oxidative phosphorylation through inhibition of ATP synthase, resulting in accumulation of cytoplasmic protons), FCCP (50 μM, a protonophore, capable of depolarizing the mitochondrial membrane leading a maximal respiration) and rotenone/antimycin A (10 μM, rotenone is a competitive inhibitor of complex I of the respiratory chain, and antimycin A inhibits mitochondrial electron transport chain complex III, both of them lead to impairing mitochondrial depolarization). Noteworthy that each arterial segment was individually normalized on a wire myograph to determine its diameter aiming to calculate the arterial surface. Finally, OCR and ECAR were referred to arterial area in mm^2.

2.10. Western blot analysis

Samples of interlobar arteries and renal cortex from STD and HFD rat kidney were snap frozen in liquid nitrogen, homogenized and lysed in buffer containing Tris-HCl (pH 7.5) 50 mmol/L, EGTA 1 mmol/L, EDTA 1 mmol/L, Triton X-100 1 % vol/vol, sodium orthovanadate 0.1 mmol/L, sodium fluoride 50 mmol/L, sodium pyrophosphate 5 mmol/L, sucrose 0.27 mol/L and protease inhibitor cocktail. Bradford assay *(Bio-Rad Laboratories, S.A, Madrid, Spain)* was used to determine the protein concentration. Protein lysates (13 μg for renal arteries and 20 μg for cortex samples) were separated in a 6,5 % polyacrylamide gel (SDS-PAGE), electrotransferred on a polyvinylidene fluoride (PVDF) membrane and probed with the following primary antibodies: GRP78 (*Cell Signaling; Danvers; MA, USA*); ATF6α, pPERK (Thr981), peIF2α (Ser52), pIRE1α (Ser724), NADPH oxidase 4 (NOX4), Manganese Superoxide Dismutase (MnSOD), cytochrome *c* oxidase subunit 4 COX-IV and peroxisome proliferator-activated receptor γ coactivator 1α (PGC-1α) (*Abcam*, *Cambridge, UK*), β-actin (*Sigma; St. Louis, MO, USA*), C/EBP homologous protein (CHOP) (*Santa Cruz Biotechnogy, Dallas, TX, USA*), as reported [10]. Horseradish peroxidase conjugated secondary antibodies was used to detect bound primary antibody, and blots were visualized with enhanced chemiluminescence, and quantified by densitometry with ImageJ free software. Protein expression levels were normalized to β-actin.

2.11. Immunohistochemistry

Immunohistochemistry for nitrotyrosine was performed on paraffin-embedded sections (5 μm) of kidney tissues fixed in 10 % paraformaldehyde in 0.1 M phosphate buffer (pH 7.4). Sections were deparaffinized, rehydrated, and incubated with 3 % hydrogen peroxide to block endogenous peroxidase activity. Antigen retrieval was carried out using citrate buffer (pH 6.0), followed by blocking of nonspecific binding. Sections were then incubated overnight at 4 °C with primary anti-nitrotyrosine antibody (1/50) (*Abcam*, *Cambridge*, UK), followed by biotinylated secondary antibodies and detection using horseradish peroxidase-conjugated streptavidin-biotin. Immunoreactivity was visualized using 3,3′-diaminobenzidine (DAB) and counterstained with Harris hematoxylin (Sigma-Aldrich, Madrid, Spain).

Immunohistochemical analysis was carried out to localize NOX4 expression in the arterial wall of kidney preglomerular arteries [42]. Renal interlobar arteries from HFD and STD rats were fixed by immersion in 4 % paraformaldehyde in sodium phosphate buffer (PBS), cryoprotected by immersion in 30 % sucrose overnight, and snap-frozen in liquid nitrogen. 5 μm thick transversal sections were obtained with a cryostat and then incubated in 10 % normal goat serum in PB containing 0.3 % Triton-X-100 and 5 % BSA for 2–3 h. NOX4 expression was determined by double immunostaining incubating renal artery sections first with a polyclonal anti-NOX4 primary antibody (1/100) (*Santa Cruz Biotechnology, Quimigen, Madrid, Spain*) and then with a mouse monoclonal anti-eNOS antibody (1:200) (*Abcam, Cambridge, UK*) for 48 h. Sections were then washed and incubated with a goat secondary serum

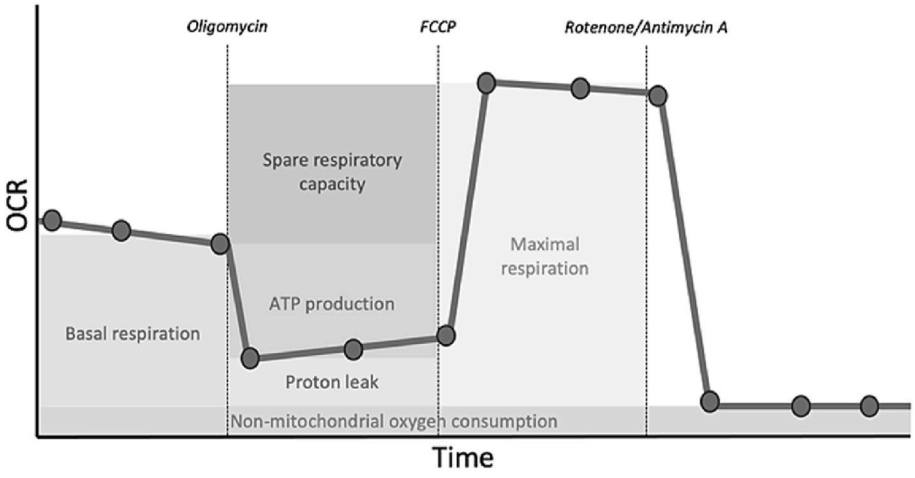

(anti-rabbit for NOX4, 1:200) (*Chemicon International Inc*) for 3 h at room temperature. The secondary antibodies used were Alexa Fluor 594 (red) and Alexa Fluor 488 (green). The slides were covered with a specific medium containing DAPI to stain all cell nuclei. Observations were made with a fluorescence microscope (Olympus IX fluorescence microscope (*Leitz Diaplan* type 020–437.035). No immunoreactivity could be detected in sections in the absence of antisera. Pre-adsorption with NOX4 proteins did not show cross-reactivity with the primary antisera.

2.12. Data presentation and statistical analysis

In the functional experiments, results are expressed as Nm^{-1} of tension or as a percent of the Phe precontraction in each artery, as means ± SEM of 6–10 arteries (1–2 artery from each animal). For $O_2^{\bullet-}$ or H_2O_2 production measurements, results are expressed in counts per minute (cpm) per mg of tissue and relative fluorescence units (RFU) per mg of tissue in arterial segments and cortex sample, respectively, as means ± SEM of 4–10 animals. Mitochondrial respiration was determined by OCR/mm^2 and $ECAR/mm^2$, as means ± SEM of 7–8 animals.

Statistically significant differences between means were analyzed by using paired or unpaired Student's *t*-test where appropriate, or one-way ANOVA followed by Bonferroni's post hoc test for multiple comparisons involving more than two groups. $P < 0.05$ were considered significant. All statistics were calculated using GraphPad Prism 8.2.1 (*GraphPad Software, Inc., San Diego, CA, United States*).

3. Results

3.1. HFD-induced obesity leads to renal structural abnormalities and kidney injury

The metabolic profile of HFD-fed rats is shown in Table 1. After 14 weeks of HF diet feeding, rats exhibited a significant increase in body weight, hyperglycemia, hypertriglyceridemia, and elevated lactate levels compared to STD (Table 1), that along with hyperinsulinemia earlier reported in this model [45] indicates a state of metabolic syndrome.

Obesity induced by HFD resulted in renal injury manifested as significantly reduced urine output indicative of oliguria (Fig. 1A), and increased protein excretion (Fig. 1B). Serum cystatin C (CYS) is a good marker of glomerular filtration rate (GFR) in humans and rodents and more sensitive than creatinine to detect minor reductions in the GFR [38,39,46]. Interestingly, CYS serum levels were found to be significantly reduced in HFD compared to STD rats (Fig. 1C) indicative of increased GFR, a hallmark of renal dysfunction in diabetes and obesity [47]. The later alterations in urine and serum renal parameters suggest an early stage of kidney functional damage. Renal functional impairment was associated with kidney structural alterations in obese rats. Kidney weight was significantly increased (Fig. 1D) despite unaltered kidney/body weight ratio in HFD obese rats. The histopathological study revealed normal glomeruli in number and size in the control STD group (Fig. 1E *left*), while kidney sections of HDF rats showed reduced number of glomeruli (Fig. E *right* and F), and significant increases in glomerular tuft area (Fig. 1E *right* and G), and Bowman's space expansion (Fig. 1E *right* and H), with a resulting increase in glomerular tuft volume (Fig. 1I) without changes in the number of cells per glomerular tuft (Fig. 1J). All these morphological changes indicate glomerular hypertrophy, a hallmark of progressing renal disease in obesity and diabetes nephropathy, associated with hyperfiltration and proteinuria.

Masson's trichrome staining of renal tissue sections revealed marked differences in glomerular and tubular architecture between control and HDF-fed rats (Fig. 1K). In the control group, glomeruli exhibited normal morphology with well-preserved capillary tufts and minimal collagen deposition, as evidenced by sparse blue staining. Renal tubules appeared structurally intact, with open lumens and little interstitial collagen, indicating preserved tubular integrity and the absence of fibrosis. In contrast, kidneys from HDF-fed rats showed pronounced glomerular alterations, including increased blue staining within the glomerular tuft, indicative of enhanced collagen deposition and glomerulosclerosis. The surrounding tubulointerstitial compartment also displayed signs of tubular atrophy and interstitial fibrosis, as shown by expanded blue-stained areas between tubules. Quantitative analysis confirmed these histological findings. The percentage of collagen within the glomerular tuft was significantly elevated in HDF-fed rats compared to controls, with values of 43.2 % ± 2.5 % versus 17.2 % ± 1.4 %, respectively ($p < 0.05$). These results demonstrate that HDF feeding induces significant glomerular and interstitial fibrotic changes in the kidney.

Table 1
Biochemical parameters of HFD and STD rats.

	STD	n	HFD	n
Body Weight (g)	383 ± 14	7	515 ± 5***	7
Age (weeks)	17	7	17	7
Glucose $_{blood}$ (mg/dl)	122 ± 9	7	184 ± 19**	7
Lactate $_{blood}$ (mg/dl)	1.3 ± 0.2	5	2.0 ± 0.2*	6
Triglycerides $_{blood}$ (mg/dl)	123 ± 11	6	281 ± 34**	7

Data represent values for weight, age, and biochemical parameters of STD and HFD rats. Data are expressed as means ± SEM for the weight of 5–7 STD rats and 7 HFD rats. Significant differences between means were analyzed by Student's *t*-test for unpaired observations. *p < 0,05; **p < 0,01; ***p < 0,001.

3.2. Endothelial dysfunction in renal preglomerular arteries from HFD-induced rats

To assess vascular function in kidney from HFD-induced obese rats, we investigated contractility and endothelial function of renal preglomerular arteries. HFD did not significantly alter internal lumen diameter of renal arteries ($l_1 = 247 \pm 14$ μm, $n = 17$ and 263 ± 14 μm, $n = 16$, in STD and HFD rats, respectively), thus initially ruling out significant arterial remodeling. However, HFD augmented contractions induced by a high K^+ depolarizing solution (KPSS) (1.58 ± 0.22 Nm^{-1}, $n = 16$, in HFD, *versus* 1.10 ± 0.13 Nm^{-1}, $n = 21$, in STD rats, $p < 0.05$, unpaired *t*-test), and reduced endothelium-dependent relaxations elicited by ACh (Fig. 2A and B), thus indicating enhanced vasoconstriction and endothelial dysfunction in preglomerular arteries.

Compromised NO synthesis and/or bioavailability induced by NOX-derived vascular oxidative stress have been involved in obesity-induced endothelial dysfunction [9,48]. Accordingly, pretreatment with the NOS inhibitor L-NOARG reduced vasodilator responses to ACh in renal arteries from control (Fig. 2C), but not from HFD rats (Fig. 2D), and the selective Nox1 inhibitor significantly improved renal endothelial relaxations in obese rats (Fig. 2F) compared to STD rats (Fig. 2E), thus suggesting the NOX1-derived oxidative stress is involved in the reduced NO-dependent endothelial relaxations of kidney preglomerular arteries in HF diet-induced obesity. On the other hand, ROS generation and peroxynitrite formation was evidenced by nitrotyrosine immunostaining in the kidney of obese rats. Nitrotyrosine immunoreactivity was localized primarily in the glomerular endothelium and in the endothelial lining of preglomerular arterioles of the HFD kidney (Fig. 3A, right panel), while slight or no immunostainig for nitrotyrosine was found in renal tissue from STD rats (Fig. 3A, left panel). Relaxations of kidney preglomerular arteries elicited by the NO donor SNAP were unaltered in arteries from HFD compared to control rats (Fig. 3B).

3.3. Mitochondrial oxidative stress, redox imbalance, and reduced vasodilator H_2O_2 contribute to endothelial dysfunction in preglomerular arteries in HFD-induced obesity

Since mitochondrial oxidative stress has been accepted as a unifying cause of diabetic-related vascular complications including nephropathy [20], we sought to elucidate the impact of obesity on mitochondrial redox homeostasis and endothelial function of kidney preglomerular

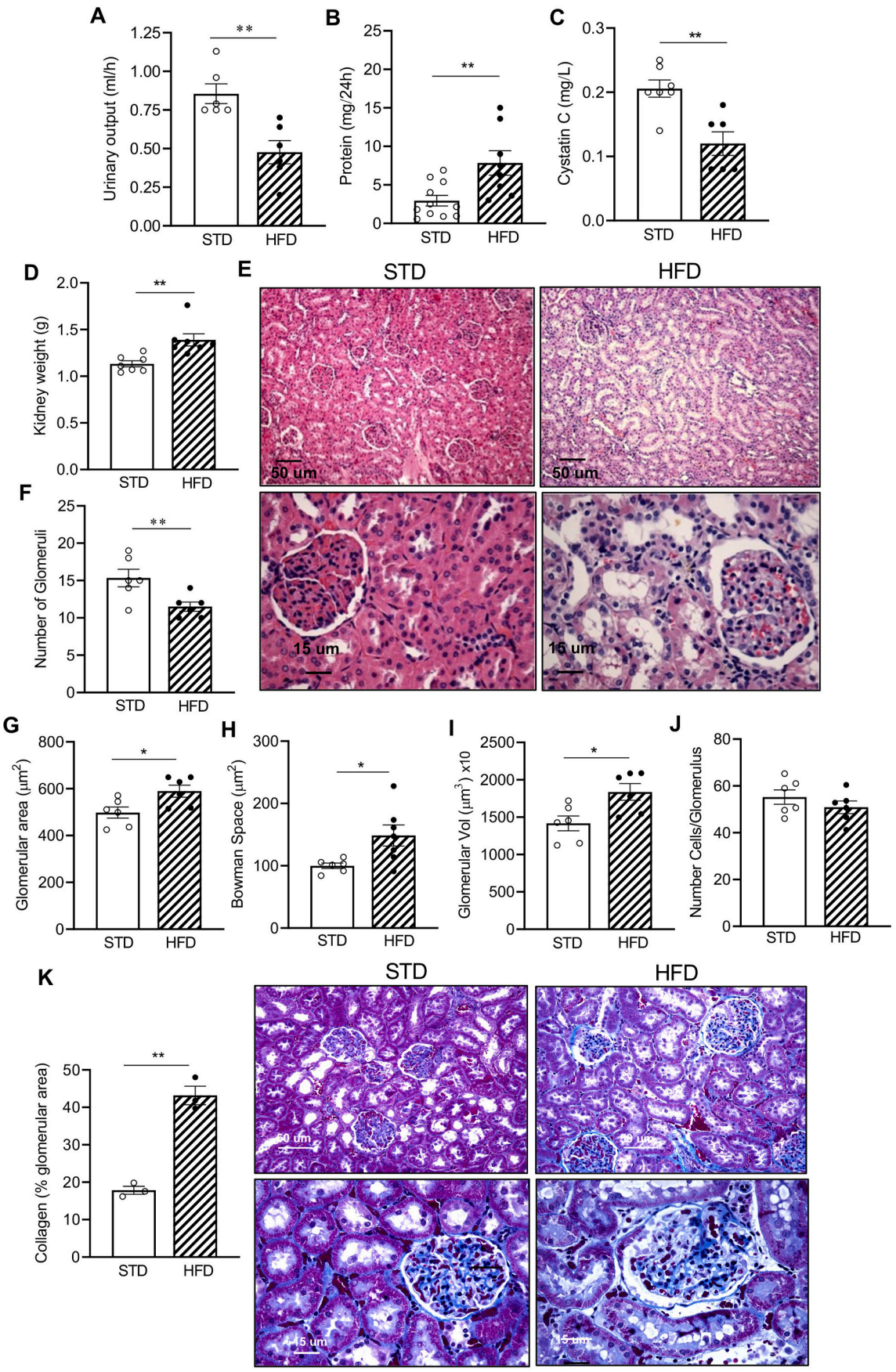

(caption on next page)

Fig. 1. HFD-induced obesity causes renal structural abnormalities and kidney injury. (A–C) Kidney function measurements showing reduced urine output (A), increased protein excretion (B) and reduced cystatin C plasma values indicative of decrease GFR (C). n = 7 HFD rats compared to 6 STD. (D–J) Morphometric histopathological study showing increased kidney weight (D) but reduced nº of glomeruli (E upper panel, F) and glomerular hypertrophy (glomerulomegaly) (E lower panel) illustrated by the increased glomerular area (G) and volume (I), and increased Bowman space area (H) without changes in the number of cells of the glomerular tuft (J) in HFD kidneys compared to STD. Measurements were taken from the average of 5 cortical fields, or 10 glomeruli cut at the vascular pole for each kidney from 6 STD and 6 HFD rats. (K) Masson's trichrome staining revealing glomerular and interstitial fibrotic changes in kidney of HFD compared to STD, depicted by the increased blue staining within the glomerular tuft and tubulointerstitial compartment. *(Left)* Quantified collagen content expressed as a percentage of the total glomerular area. $P < 0.05$; $p < 0.01$ Student's *t*-Test for impaired observations.

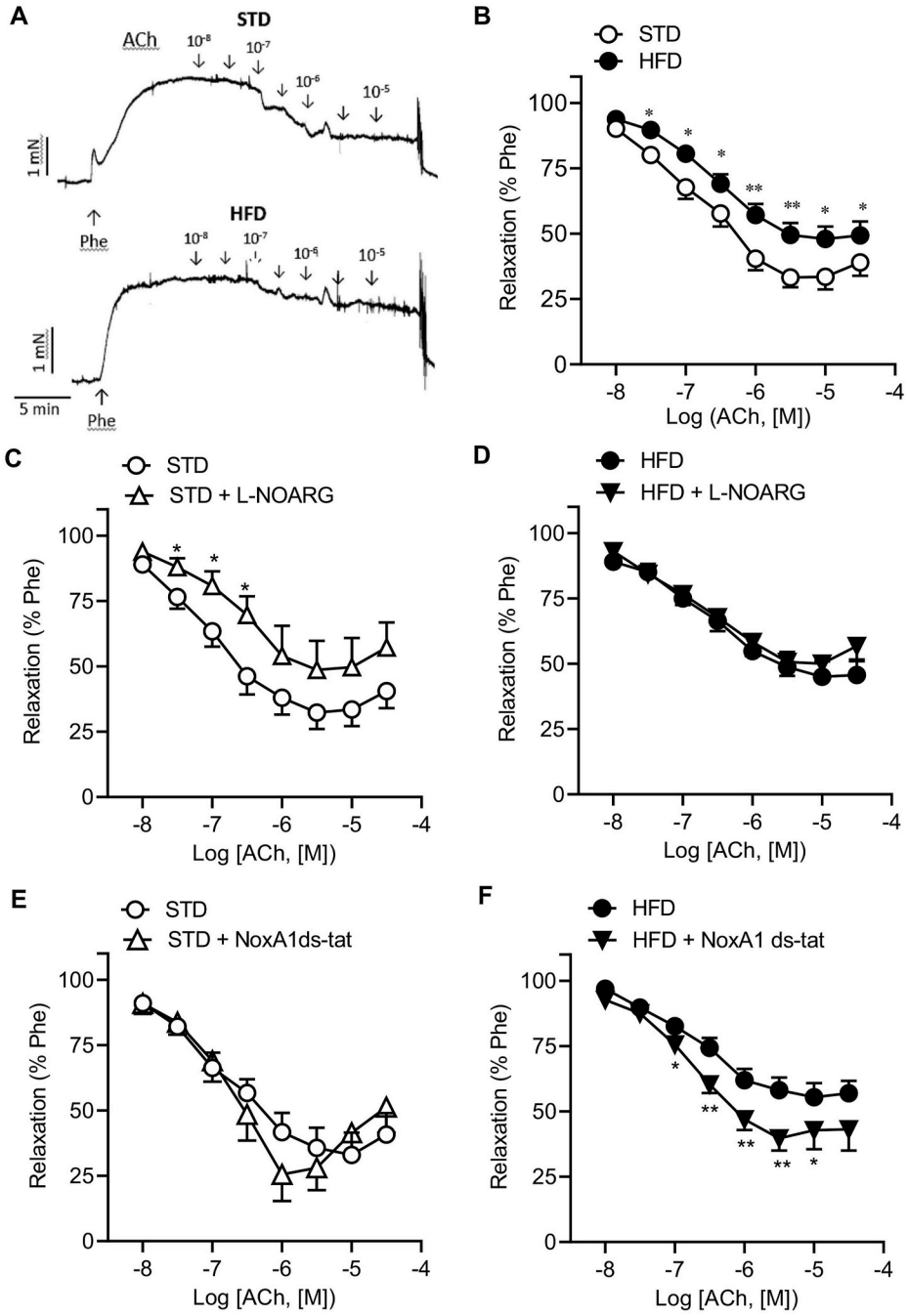

Fig. 2. NOX1-derived ROS are involved in NO-mediated endothelial dysfunction of kidney preglomerular arteries from obese rats (A) Isometric force recordings showing the relaxations to the endothelial agonist ACh in preglomerular renal arteries from STD (upper) compared to HFD rats (down). (B) Average relaxations to ACh in arteries from STD and HFD rats. (C–F) Average relaxations to ACh in renal arteries after treatment with the nitric oxide (NO) synthase (NOS) inhibitor, L-NG-nitro-arginine (L-NOARG) (C–D), and with the NOX1 inhibitor NoxA1 ds-tat (E–F). Results are expressed as a percentage of the increase in tension induced by Phe (1 μM). Data are presented as the mean ± SEM of 7–9 arteries of STD and 8–9 arteries of HFD. Significant differences between means were analyzed by Student's *t*-test for unpaired observations. *$p < 0.05$, **$p < 0.01$ *versus* STD.

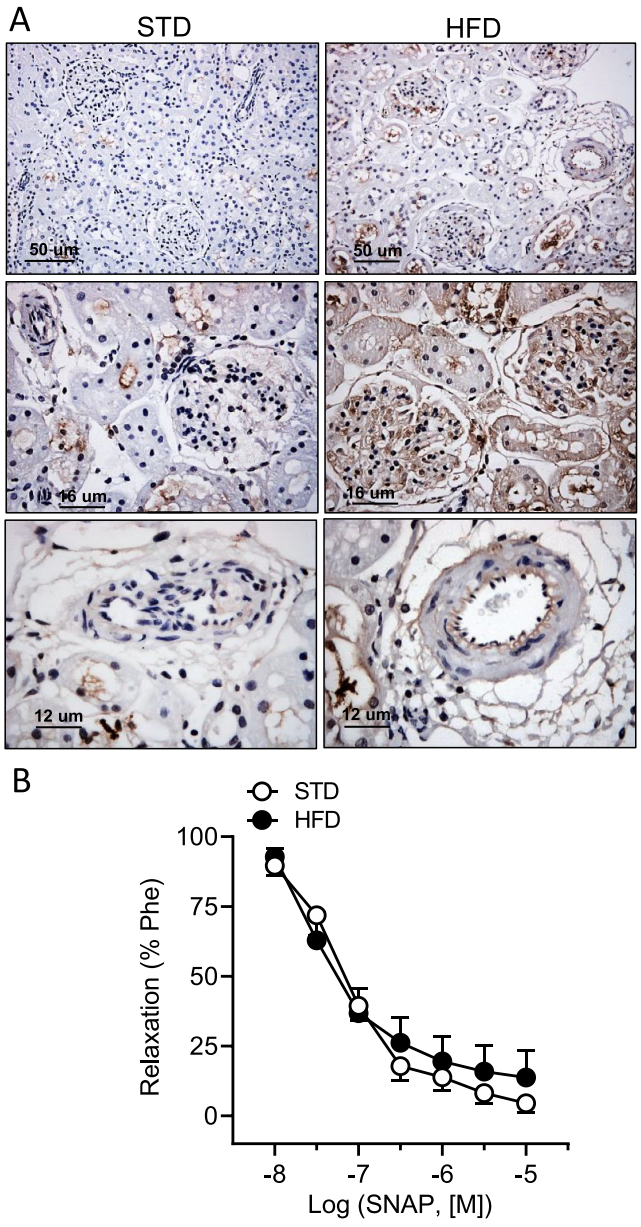

Fig. 3. Augmented peroxynitrite and preserved exogenous NO-mediated relaxations in kidney preglomerular from HFD-induced *obese rats.* (A) Nitrotyrosine immunostaining for peroxynitrite was enhanced in renal cortex, mostly in the glomerular tufts and endothelial lining of renal arterioles from HFD (right) compared to STD (left) rats. Sections are representative of n = 3 STD and n = 3 HFD rats. (B) Average relaxations to the NO donor SNAP in preglomerular arteries from STD and HFD rats. Data are presented as the mean ± SEM of arteries of 4 STD and 4 HFD.

arteries. mtROS levels were measured with MitoSOX (superoxide) and Amplex red (H_2O_2) fluorometric assays in kidney tissues from STD and HFD. While renal arteries from HFD-fed rats exhibited elevated mtROS levels compared to STD (Fig. 4A), this effect was not observed in renal cortex (Fig. 4B). H_2O_2 participates in endothelial cell signaling and has been involved along with NO in the endothelium-dependent vasodilation of kidney arteries [42,49]. Measurement of basal H_2O_2 levels revealed a significant decrease in both arteries (Fig. 4C) and renal cortex (Fig. 4D) from HFD rat kidney. Despite increased NOX1-derived ROS production (Fig. 2F), global NOX-derived H_2O_2 was not augmented in either kidney arteries (Fig. 4E) or cortex (Fig. 4F) from HFD rats, as depicted by the unchanged levels of NADPH activity-dependent ROS levels. Interestingly, treatment with the mitochondria-targeted antioxidant mitoTempo reduced ACh-induced arterial vasodilation in STD animals (Fig. 4G), while improving endothelial relaxations in kidney arteries from obese rats (Fig. 4H). Together, these results suggest that enhanced mitochondrial $O_2^{\bullet-}$ along with reduced vasodilator H_2O_2, contribute to the observed endothelial dysfunction in kidney preglomerular arteries in HF diet-induced obesity.

3.4. HFD-induced obesity down-regulates NOX4 and PGC1α expression in kidney preglomerular arteries

To further investigate the mitochondrial redox status of kidney vascular and cortical tissues in diet-induced obesity, expression levels of ROS generating enzymes and regulators of mitochondrial antioxidant defenses were determined by Western Blot analysis in STD and HFD rats. NOX4, a mitochondrial enzyme highly expressed in the kidney that directly generates H_2O_2, is a physiological source of endothelium-derived vasodilator H_2O_2 in renal arteries [42]. The present findings demonstrate that expression of NOX4 is confined to the renal arterial endothelium wherein it co-localizes with eNOS in both control and obese rats kidney (Fig. 5A), and that NOX4 protein levels are significantly reduced in both renal arteries and cortex of HFD rats (Fig. 5B and E). Positioned strategically within the mitochondria, MnSOD converts harmful $O_2^{\bullet-}$, a byproduct of the mitochondrial ETC, into H_2O_2 that rapidly diffuses out of the mitochondria. Protein expression of MnSOD was unaltered in renal arteries (Fig. 5D) but increased in renal cortex (Fig. 5G) of obese animals. The transcriptional coactivator PGC-1α is a regulator of mitochondrial biogenesis that also regulates mitochondrial antioxidant systems in vascular endothelial cells [50]. PGC-1α protein levels were significantly reduced in both arteries and cortex from HFD rat kidney (Fig. 5C and F), suggesting impaired kidney mitochondrial biogenesis and dysregulation of endothelial antioxidant systems in HF diet-induced obesity.

3.5. HFD-induced obesity enhances mitochondrial respiration in kidney preglomerular arteries

Mitochondrial dysfunction in metabolic diseases is manifested by alterations in OXPHOS leading to mitochondrial oxidative stress. Having observed considerable changes in mtROS production and variations in antioxidant defenses expression in kidney arteries from obese rats, the impact of obesity on vascular mitochondrial bioenergetics was next assessed in freshly isolated intact kidney preglomerular microarteries by using a Seahorse Analyzer and a *Mito-stress* protocol for real-time measurements of oxygen consumption and extracellular acidification (Fig. 6). Interestingly, the bioenergetic profile of preglomerular arteries was markedly increased in HFD rats (Fig. 6A). Basal respiration and oxygen consumed for ATP synthesis obtained following oligomycin addition, were significantly heightened in arteries from obese rats (Fig. 6A–C), along with increased maximal respiration induced by the uncoupling agent FCCP (Fig. 6A and D), and augmented proton leak (Fig. 6A and E). These data align with the previously observed increase in mitochondrial ROS generated as by-products of the ETC enhanced activity. Oxygen consumed for non-mitochondrial respiration was also found to be increased after adding rotenone and antimycin A (Fig. 6A and F), and probably derived from prooxidant and pro-inflammatory enzymes such as NADPH oxidases and cyclooxygenases [13,14].The rise in mitochondrial respiration was concomitant with the increased levels of protons indicating augmented glycolytic activity and subsequent increase in extracellular acidification in preglomerular arteries from HFD rats (Fig. 6G). Consistent with the enhanced mitochondrial bioenergetic profile, expression of mitochondrial ECT complex IV (COX-IV) was increased in renal arteries of HFD-fed animals (Fig. 6H).

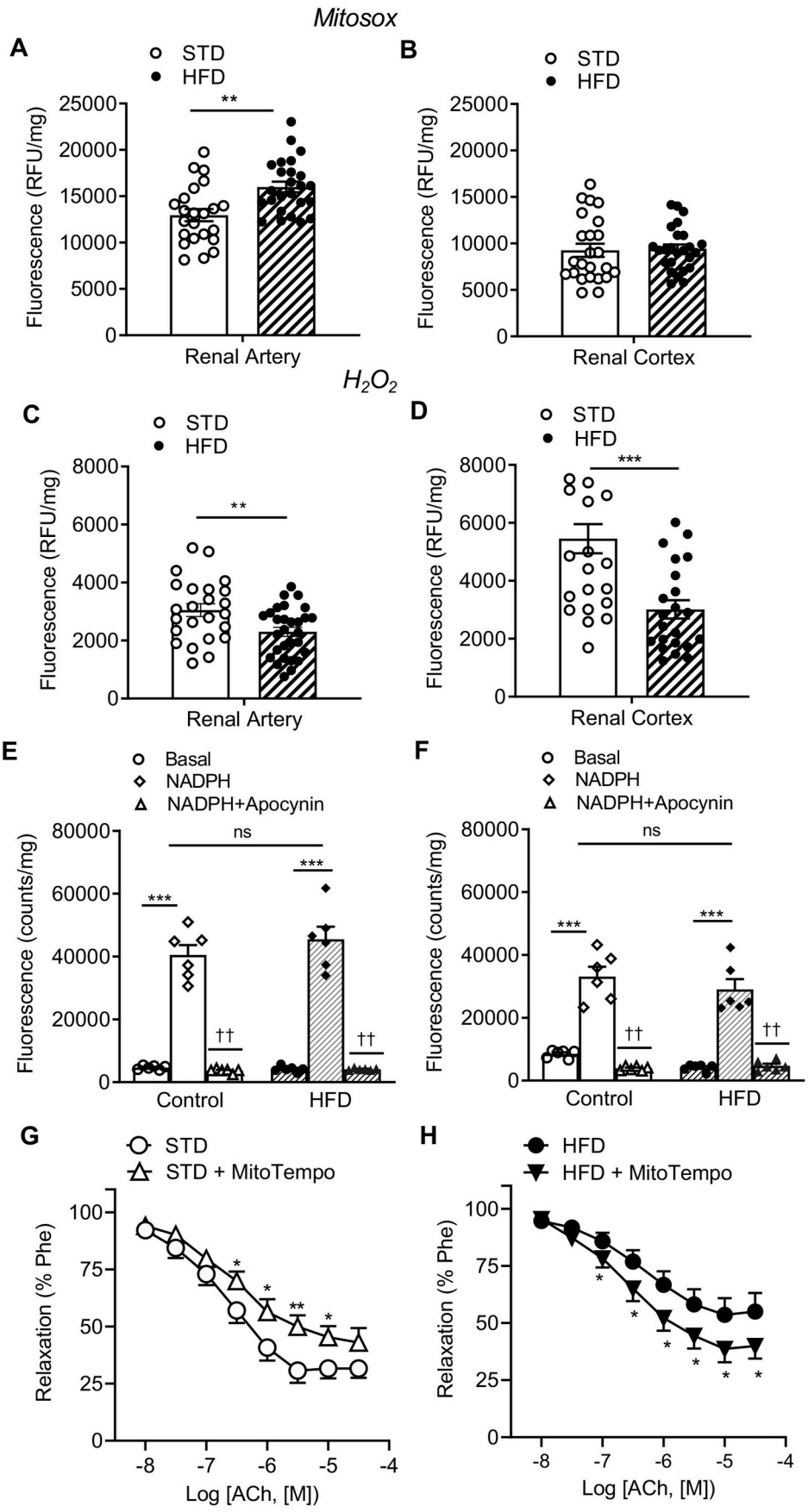

(caption on next page)

Fig. 4. Mitochondrial ROS imbalance contributes to renal endothelial dysfunction in HFD-induced *obesity* (A–B) Basal mitochondrial ROS ($O_2^{\bullet-}$) measured by MitoSOX fluorescence, and (C–F) basal H_2O_2 (C,D) and NADPH-stimulated H_2O_2 (E,F) production measured by AmplexRed fluorescence in renal arteries (A–E) and cortex (B–F) from STD and HFD rats. Data are presented as mean ± SEM from 24 to 25 arteries and 26–27 cortex samples form 6 STD and 6 HFD (A, B); 24–26 arteries and 23–25 cortical samplex from 9 STD and 9 HFD rats (C,D); 6 arteries and 6 cortex samples of 4 STD and 4 HFD (E,F). Significant differences between means were analyzed by Student's *t*-test for unpaired observations. $^{**}p < 0.01$; $^{***}p < 0.001$ versus STD group (A–D) and One-way ANOVA followed by Bonferroni test (E,F). $^{***}p < 0.001$ *vs* basal levels, $^{\dagger\dagger}p < 0.01$vs NADPH-stimulated; (G,H) Average relaxations to ACh in the absence and after treatment with the mitochondrial antioxidant mitoTempo in control STD (G) and HFD (H) renal arteries. Results are expressed as a percentage of the pre-contraction induced by Phe (0.1–0.3 μM). Data are presented as the mean ± SEM of 6–8 arteries from 6 STD and 6 HFD rats. Significant differences between means were analyzed by Student's *t*-test for paired observations. $^{*}p < 0.05$; $^{**}p < 0.01$ versus control arteries in the absence of MitoTempo.

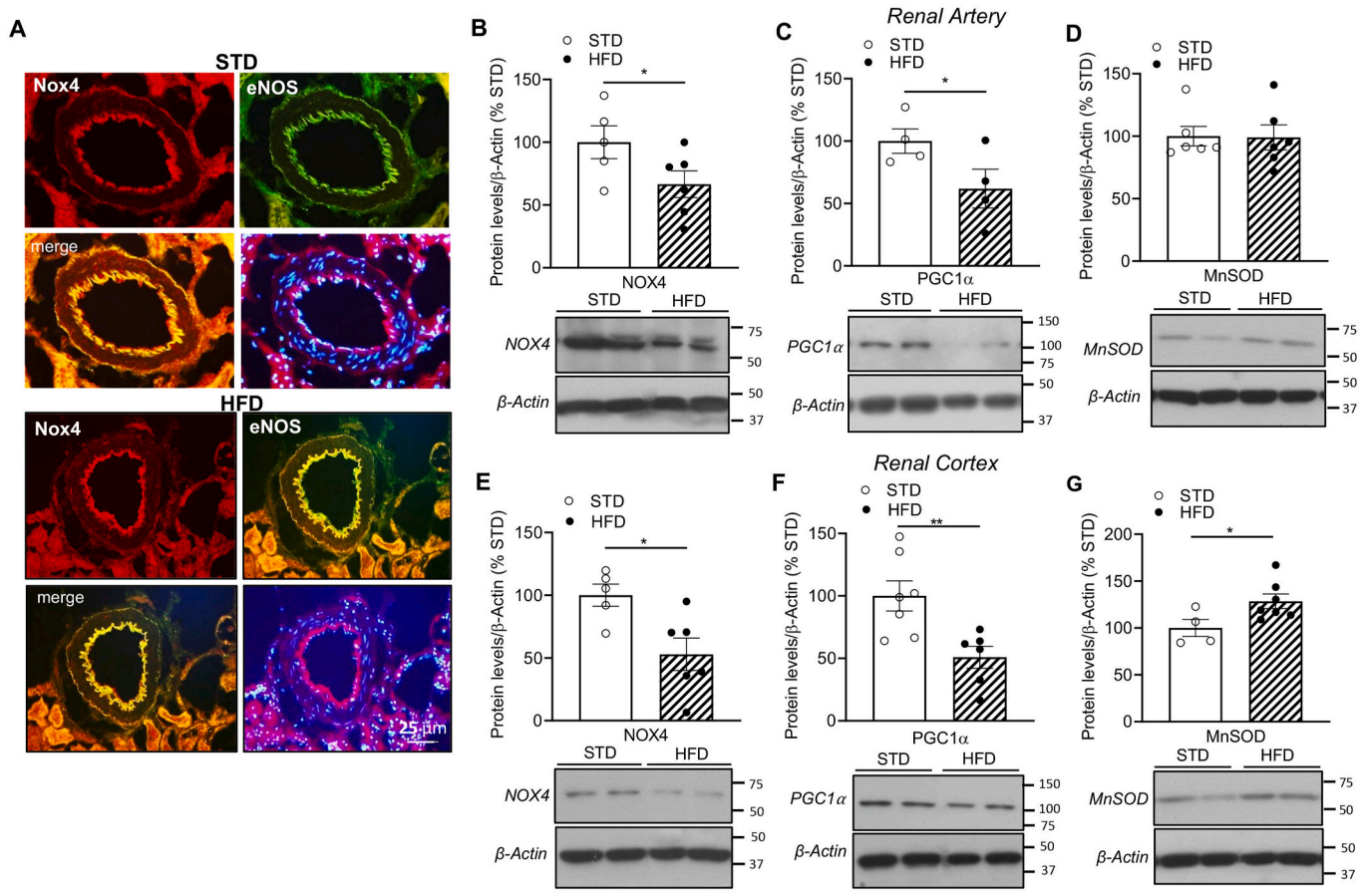

Fig. 5. Obesity induced by HFD downregulates PGC-1α and NOX4 in kidney tissues (A) Immunofluorescence for NOX4 protein (red) is distributed throughout the endothelial lining of the renal arteries in STD (upper panels) and HFD (lower panels) groups. The endothelial cell layer is visualized using the anti-eNOS marker (green). Double immunofluorescence labeling for eNOS and NOX4 shows colocalization in the renal endothelium (yellow). Nuclei are stained with DAPI (blue). Scale bars indicate 25 μm. Sections are representative of n = 3 STD and n = 3 HFD rats. (B–G) Western blot analysis of NOX4, PGC-1α and MnSOD expression in samples of preglomerular renal arteries (B–D) and cortex (E–G) showing that expression of NOX4 and PGC-1α was decreased in both renal arteries and cortex of HFD rats, while MnSOD was not changed in renal arteries, but increased in renal cortex from obese animals. Data are shown as the mean ± SEM of 4–7 STD and 4–7 HFD rats. Significant differences between means were analyzed by using unpaired *t*-test. $^{*}P < 0.05$, $^{**}P < 0.01$ versus STD.

3.6. ER stress induces endothelial dysfunction and blunts adrenergic vasoconstriction in kidney preglomerular arteries

Because ER stress has been involved in the pathogenesis of endothelial dysfunction in the context of obesity [33], and in proteinuric kidney disease, ER stress status in renal tissues affected by HFD-induced obesity was next assessed. A significant increase in expression of some of the activated sensors of the UPR pathway such as pPERK, peIF2α, and pIRE1α was found in kidney arteries (Fig. 7A, B, and D), and of the chaperone BiP and peIF2α, and pIRE1α in renal cortex (Fig. 7E–G, H and I) of obese rats compared to the control group, while ATF6α was decreased in renal arteries (Fig. 7C) but increased in renal cortex (Fig. 7C) from HFD animals. The latter may be attributed to the complexity of ER stress activation, given that different UPR pathways can be selectively stimulated together with suppression of others [25]. Expression of the indicator of UPR-apoptosis activation, CHOP, exhibited a non-significant upwards trend (Fig. 7J).

To further investigate the impact of ER stress on vascular function of kidney preglomerular arteries, a rat model of chemically-induced ER stress with tunicamycin was stablished. Increased expression/activation of various ER stress markers was found in both renal arteries and cortex of rats treated with tunicamycin (Fig. S2 A-I), thus validating the ER stress model in the kidney. Vascular dysfunction in kidney preglomerular arteries from tunicamycin-treated rats was depicted by the reduced contraction induced by the α_1-adrenergic agonist phenylephrine (Fig. 8A) along with the blunted NO-mediated vasodilation in response to ACh indicative of endothelial dysfunction in renal preglomerular arteries from rats with ER stress (Fig. 8B and D). Vasorelaxation elicited by the β-adrenergic agonist isoprenaline remained unchanged (Fig. 8C).

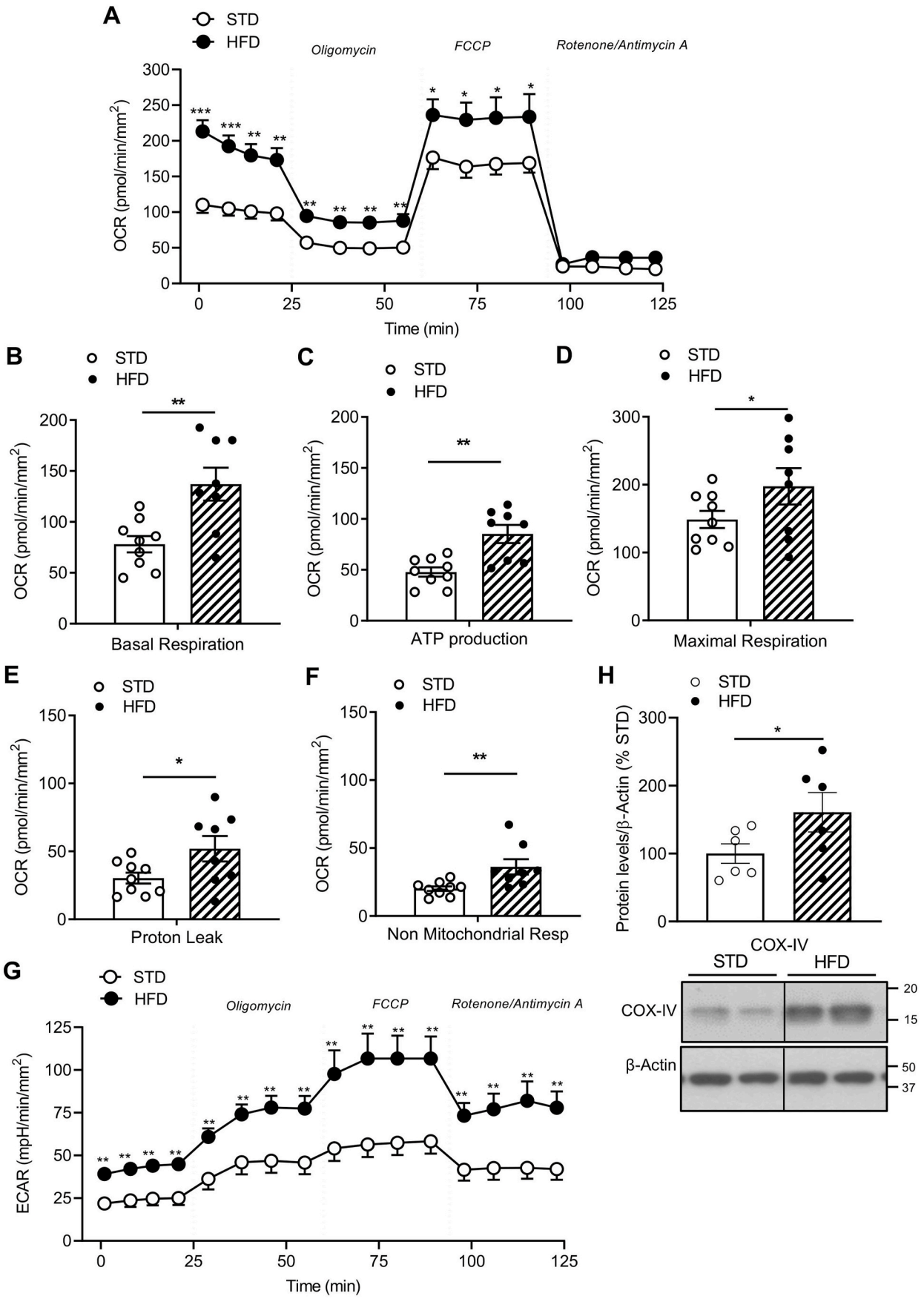

(caption on next page)

Fig. 6. Obesity enhances mitochondrial bioenergetics in kidney preglomerular arteries (A–G) The MitoStress test was performed on freshly isolated preglomerular arterial segments using Seahorse technology to measure the oxygen consumption rate (OCR) and extracellular acidification rate (ECAR) in STD and HFD rats. Sequential injections of oligomycin, FCCP, and rotenone/antimycin A were administered to assess mitochondrial function (A). Renal arteries from HFD rats exhibited increased basal respiration (A and B), ATP production (A and C), maximal respiration (A and D), proton leak (A and E), non-mitochondrial respiration (A and F), and ECAR (G) compared to STD. Results are expressed as pmol O_2/min (OCR) or mpH/min (ECAR) values and referred to the arterial segment surface in mm^2. (H) Western Blot analysis showing increased expression of mitochondrial ECT complex IV (COX-IV). Data are shown as means ± SEM of 7–8 STD and 7–9 HFD arteries from n = 7 rats. Significant differences between means were analyzed by using unpaired *t*-test. *P < 0.05, **P < 0.01, ***p < 0.001 versus STD.

To assess the impact of NOX-derived oxidative stress on renal endothelial function under ER stress conditions, the effect of the non-selective NOX inhibitor apocynin was examined on renal preglomerular arteries from tunicamycin-treated rats. Apocynin inhibited ACh-induced endothelial relaxations in control arteries (Fig. 8E), without affecting relaxations in the ER stress group (Fig. 8F), indicating that relaxations mediated by endothelial NOX-derived ROS in renal preglomerular arteries [42] are lost in ER stress rats. Accordingly, lucigenin chemiluminescence revealed an elevation in NADPH-induced ROS production in renal cortex but not in renal arteries of tunicamycin-treated rats compared to controls (Fig. 8G and H). The NADPH-dependent ROS increase was reversed by apocynin in control arteries, but this reversal was not observed in ER stress renal arteries (Fig. 8G). In contrast, apocynin effectively reduced elevated NADPH-dependent ROS levels in renal cortex samples from tunicamycin-treated rats. In summary, these data suggest that ER stress blunts the release of endothelial NOX-derived relaxing ROS, presumably H_2O_2 in renal preglomerular arteries, but induces NOX-derived oxidative stress in renal cortex.

3.7. *Impaired REDOX balance and reduced mitochondrial H_2O_2 contribute to kidney endothelial dysfunction in chemically-induced ER stress*

Involvement of mtROS and mitochondrial oxidative stress in endothelial dysfunction induced by ER stress was further investigated. Endothelium-dependent vasodilation elicited by ACh was reduced by the mitochondrial $O_2^{\bullet-}$ scavenger mitoTempo in control rats (Fig. 9A), but this effect was reversed in arteries from ER stress rats (Fig. 9B). Levels of both mitochondrial $O_2^{\bullet-}$ and H_2O_2 were significantly reduced in ER stress preglomerular arteries (Fig. 9C and D), thus suggesting the loss of physiological vasodilator mtROS [42], likely H_2O_2. In renal cortex from tunicamycin-treated rats, unchanged mitochondrial $O_2^{\bullet-}$ but reduced H_2O_2 levels were also found (Fig. 9G and H). To further investigate the impact of ER stress on antioxidant defense status of kidney tissues, protein expression of NOX4 and MnSOD was assessed. In line with the decreased H_2O_2 production, ER stress led to the reduction in NOX4 expression in both renal arteries (Fig. 9E) and cortex (Fig. 9I) of ER stress rats compared to controls. Moreover, there was a significant increase in MnSOD levels in renal arteries (Fig. 8F), while a decrease was observed in the renal cortex (Fig. 9J) from tunicamycin-treated rats.

3.8. *ER stress enhances mitochondrial respiration in kidney preglomerular arteries*

To further investigate redox changes and the impact of ER stress on kidney vascular bioenergetics, mitochondrial respiration was assessed in renal preglomerular intact arteries from the ER stress rat model, revealing that ER stress led to an elevation in basal oxygen consumption (Fig. 10A and B), and oxygen consumed for ATP production (Fig. 9A and C). However, maximal respiration induced by FCCP (Fig. 10A and C) was unchanged, but the increase in basal respiration resulted in a reduced spare respiratory capacity (Fig. 10A and E), which is crucial during other stress requirements. In tunicamycin-treated rats, there was a significant elevation in the ECAR (Fig. 9F), indicating an augmentation of glycolytic activity under ER stress conditions.

4. Discussion

Mitochondrial dysfunction is involved in the pathogenesis of obesity and CKD, and oxidative stress derived from mtROS plays a pivotal role in the microvascular complications of both obesity and type 2 diabetes. The results presented here elucidate a complex molecular interplay involving redox imbalance, impaired mitochondrial function, and ER stress in the context of kidney vascular dysfunction associated with obesity-induced renal injury. We demonstrate that endothelial dysfunction of renal preglomerular arteries in diet-induced obese rats or under ER stress conditions is linked to impaired vascular mtROS generation featured by increased vasoconstrictor ROS and a reduction of vasodilator H_2O_2 along with downregulation of NOX4 and of the mitochondrial biogenesis marker PGC1α. These changes are associated with an adaptive enhancement of arterial mitochondrial bioenergetics likely related to hemodynamic changes in kidney preglomerular arteries to supply function of injured glomeruli in obesity.

Obesity and overweight were early associated with impaired endothelium-dependent vasodilation in clinical studies [51], compromised NO synthesis and bioavailability due to oxidative stress being key factors in the pathogenesis of endothelial dysfunction, an early pathogenic event in CVD [48,52]. Accordingly, NO-mediated vasodilation was found to be impaired in kidney preglomerular arteries from diet-induced obese rats and selective inhibition of NOX1 partially restored endothelial vasodilatation thus suggesting that NOX1-derived superoxide blunts relaxations involving NO, consistent with that found in genetically obese rats [9]. Moreover, we demonstrate here that HFD induces nitrosative stress in the kidney due to the interaction of augmented superoxide with NO thus generating the strongly oxidative and toxic peroxynitrite radical. Peroxynitrite accumulation in the kidney glomerular and arteriolar endothelium, as depicted by the nitrotyrosine immunostaining, causes oxidative damage to DNA, lipids and proteins, eNOS uncoupling, enhanced apoptosis and tissue injury and inflammation. However, relaxations induced by exogenous NO were preserved in preglomerular arterioles of HFD-induced obese rats, consistent with the reported enhanced sensitivity to NO of coronary arterioles developed to maintain NO-mediated dilatation in HFD-induced obesity [45].

On the other hand, the present data further demonstrate that an imbalance in vascular mtROS levels also contributes to renal endothelial dysfunction in obesity. Thus, blunted endothelium-dependent relaxations in kidney preglomerular arteries of obese animals were associated with increased levels of mtROS, consistent with the involvement of mitochondria-derived oxidative stress in endothelial dysfunction, as earlier reported for human arterioles of type 2 diabetic patients [35]. The critical role of mtROS in endothelial dysfunction has also been evidenced by the improved vascular function after treatment with mitochondria-targeted antioxidants demonstrated in preclinical studies [53,54] and human trials [55]. In diabetic patients, altered mitochondrial dynamics in endothelial cells affects eNOS activation and NO bioavailability via excess mtROS which leads to endothelial dysfunction [56]. However, whereas the mitochondrial-targeted antioxidant mitoTempo improved endothelial function in arterioles from diabetic patients [35], in the present study treatment with mitoTempo revealed differential effects both inhibiting and improving relaxant responses in kidney preglomerular arteries from control and obese rats, respectively. These results demonstrate an impaired mitochondrial redox balance with augmented constrictor in detriment of vasodilator mtROS in kidney arteries from HFD rats, which is confirmed by the increased $O_2^{\bullet-}$ levels

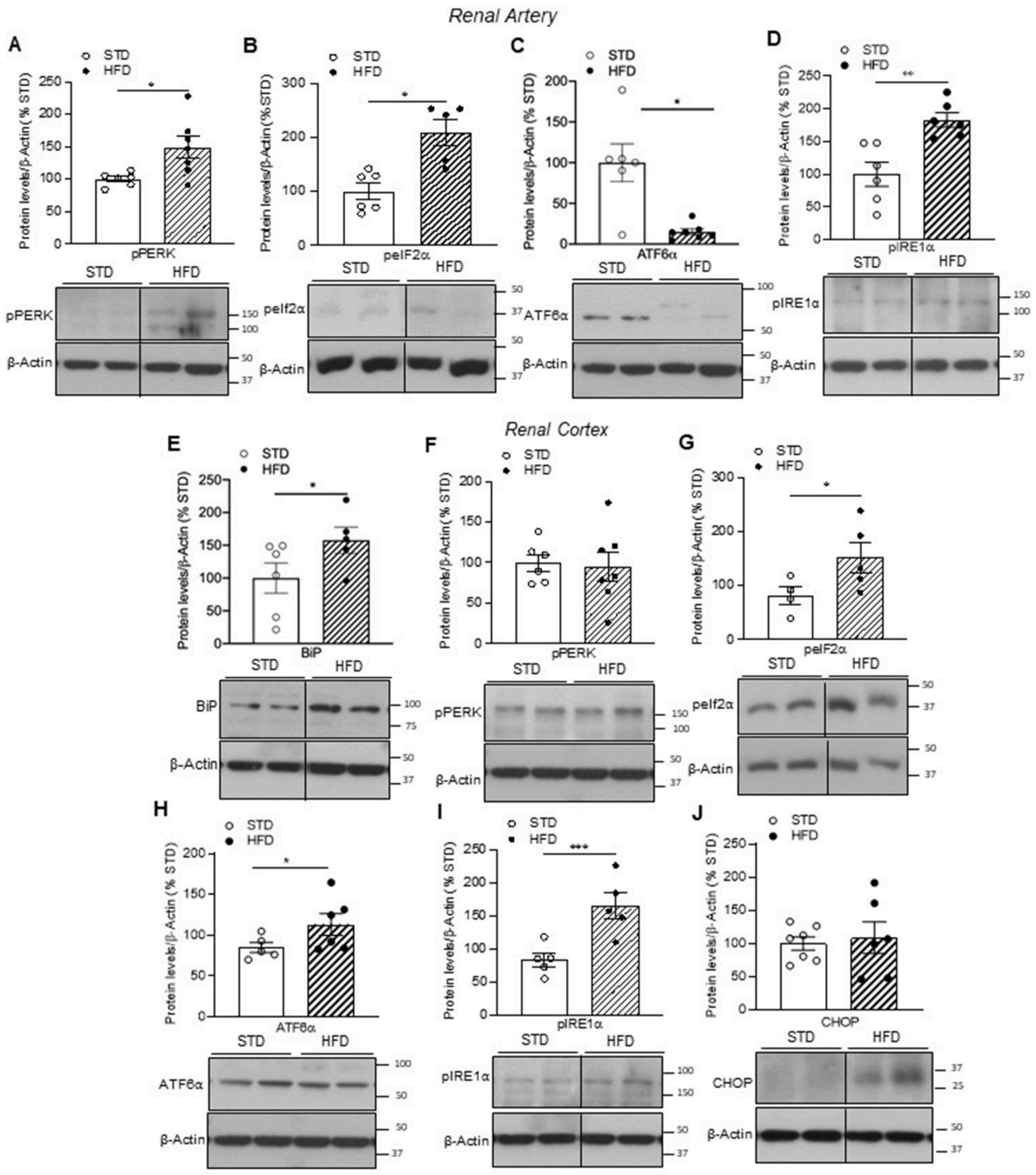

Fig. 7. ER stress markers in kidney tissues of HFD-induced obese rats Western blot analysis showing the expression of ERS markers in kidney preglomerular arteries (A–D) and cortex (E–J) from HFD-fed rats. The expression of pPERK (A), peIF2α (B) and pIRE1α (D) was increased in renal arteries from HFD rats, while ATF6α (C) was decreased. Protein expression of BiP (E), peIF2α (G), ATF6α (H), pIRE1α (I) were significantly augmented, while CHOP showed a trend to increase (J) in renal cortex from HFD rats. Data are shown as the mean ± SEM of 4–7 STD and 5–7 HFD rats. Significant differences between means were analyzed by using unpaired *t*-test. *P < 0.05, ***P < 0.001 versus STD.

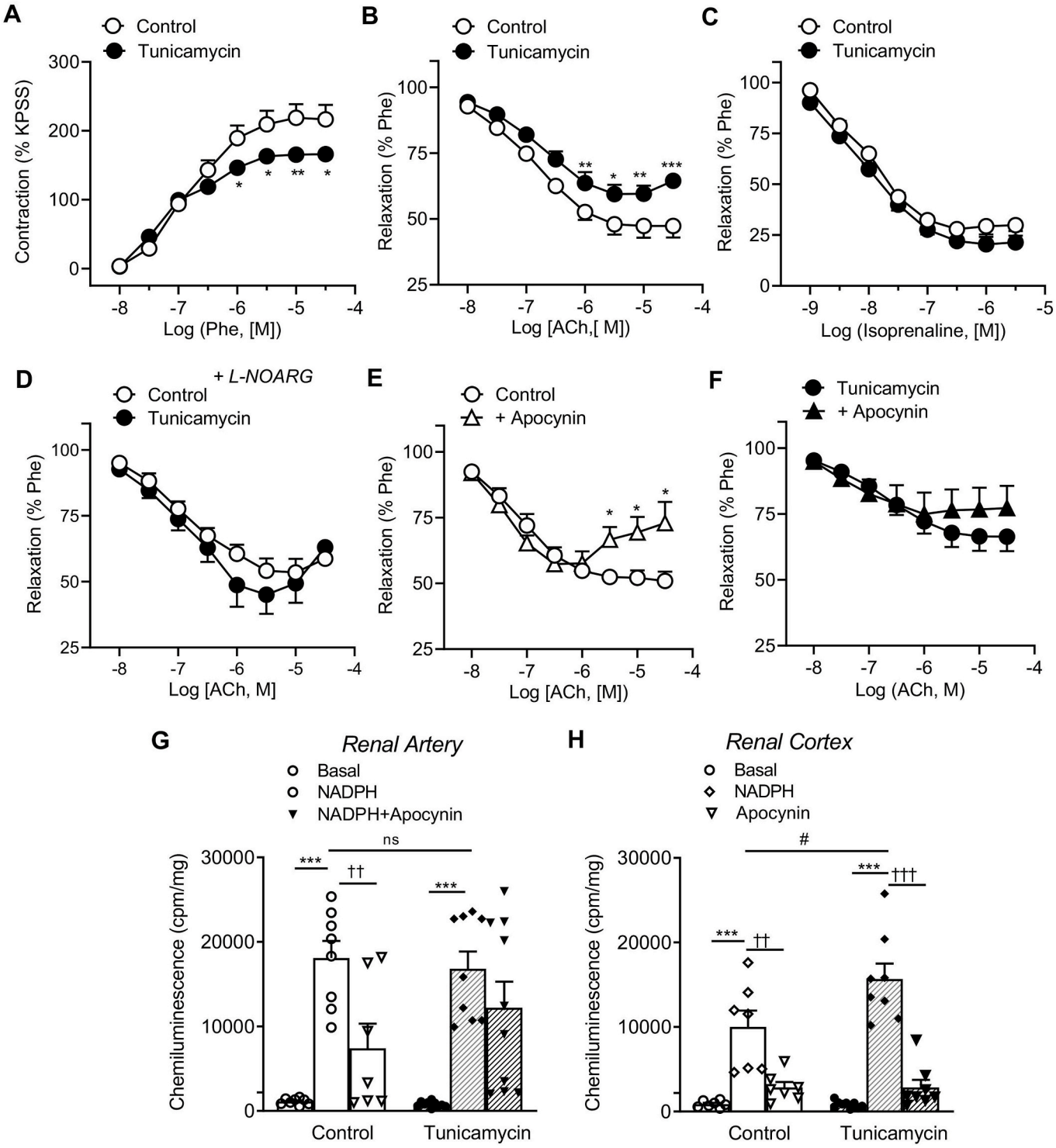

Fig. 8. Vascular dysfunction in kidney preglomerular arteries from ER stress rats (A) Contractions to the α_1-adrenergic agonist Phe, (B) relaxations to the endothelial agonist ACh and (C) the β-adrenoceptor agonist isoprenaline in renal arteries from control and the ERS inductor tunicamycin *in vivo*-treated rats. (D) Average relaxations to ACh in presence of the NOS inhibitor L-NOARG in control and tunicamycin-treated rats. (E–F) Effect of apocynin on ACh-induced relaxations in renal arteries of (E) control and (F) tunicamycin-treated rats incubated with the NOX inhibitor apocynin. Contractile results are expressed as a percentage of KPSS (A), relaxation is expressed as percentage of the increase in tension induced by Phe (0.1–0.3 μM) (B–F). Data are presented as the mean ± SEM of 6–28 arteries of control and 6–30 of tunicamycin-treated rats. Significant differences between means were analyzed by Student's *t*-test for paired observations. *$p < 0.05$, **$p < 0.01$, ***$p < 0.001$ versus control. (G–H) ROS production measured by lucigenin-enhanced chemiluminescence, under basal, NADPH-stimulated and NADPH-induced in presence of the NOX inhibitor apocynin conditions in renal arteries (G) and cortex (H) from control and tunicamycin-treated rats. Data are presented as mean ± SEM from 7 to 8 control arteries and 6–8 cortex samples from 4 control and 5 tunicamycin-treated rats. Significant differences between means were analyzed by Student's *t*-test for unpaired observations. ***$p < 0.001$ versus basal conditions; $^{\dagger}p < 0.05$, $^{\dagger\dagger}p < 0.01$, $^{\dagger\dagger\dagger}p < 0.001$ versus NADPH stimulation; $^{\#}p < 0.05$ versus control group.

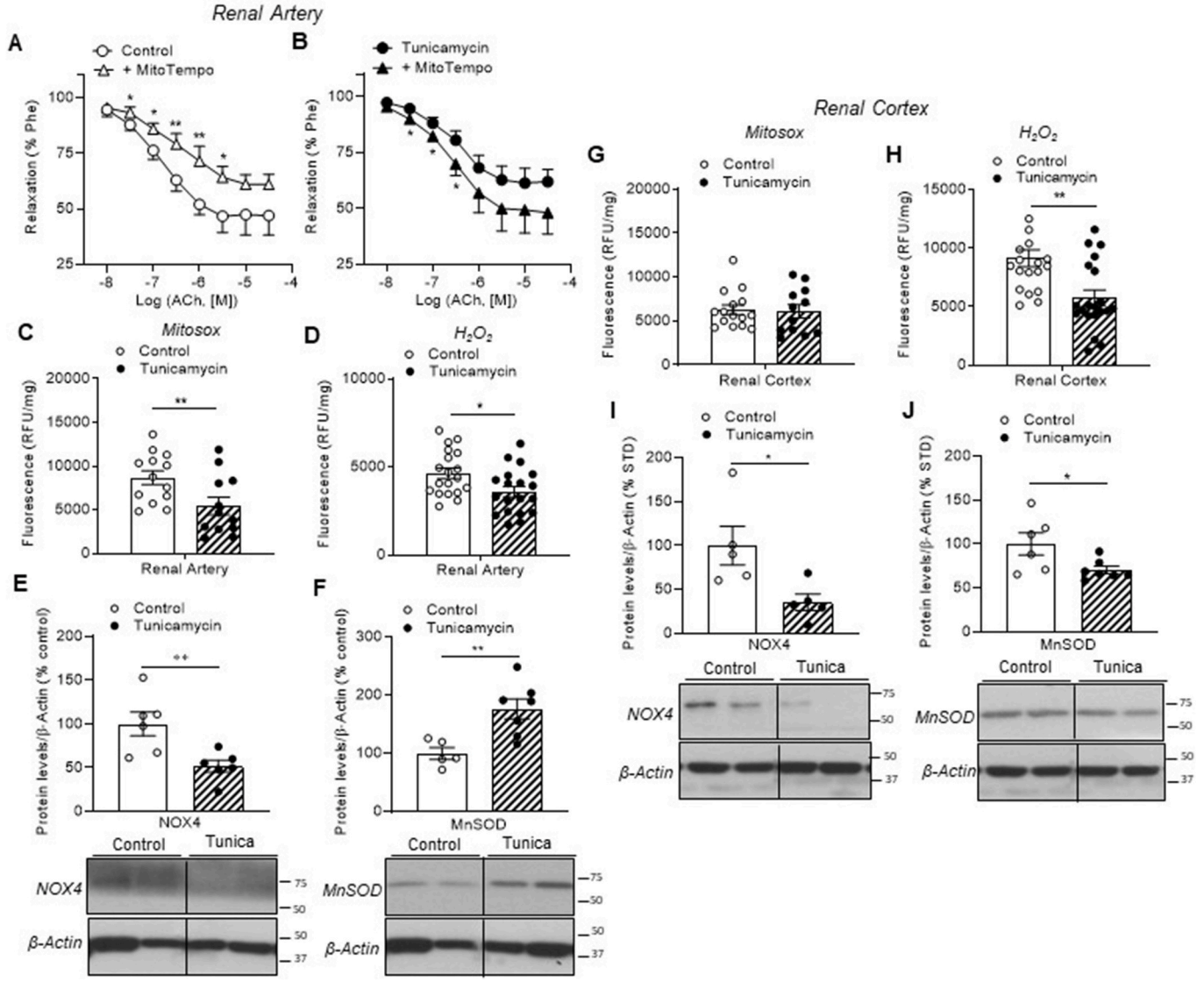

Fig. 9. Reduced NOX4 expression and lower H_2O_2 levels contribute to renal endothelial dysfunction in tunicamycin-induced ER stress. (A–B) Average relaxations to ACh after treatment with the mitochondrial antioxidant mitoTempo in renal arteries of control (A) and tunicamycin treated rats (B). The results are expressed as a percentage of the pre-contraction induced by Phe (0.1–0.5 μM). Data are presented as the mean ± SEM from 10 to 12 arteries from 6 control and 7 ER stress rats. Significant differences between means were analyzed by Student's *t*-test for paired observations. *p < 0.05; **p < 0.01 versus arteries without MitoTempo. (C and G) Mitochondrial ROS ($O_2^{\bullet-}$) measured by MitoSOX fluorescence, and (D and H) H_2O_2 production measured by AmplexRed in renal arteries (C–D) and cortex (G–H) from control and tunicamycin treated rats. Data are presented as mean ± SEM from 13 to 14 arteries and 14–16 cortex samples from 4 control and 4 tunicamycin-treated rats. Significant differences between means were analyzed by Student's *t*-test for unpaired observations. *p < 0.05 **p < 0.01 *versus* control. (E-F and I-J) Western blot analysis of NOX4 and MnSOD expression in samples of preglomerular renal arteries (E–F) and cortex (I–J) of control and tunicamycin-treated rats. Data are shown as the mean ± SEM of 5–6 control and 6–7 tunicamycin treated rats. Significant differences between means were analyzed by using unpaired *t*-test. *P < 0.05, **P < 0.01 versus controls.

measured by mitoSOX along with the reduction in vasodilator H_2O_2 levels measured by Amplex Red.

Although endothelial cells have a relatively lower mitochondrial content compared to cells that depend on aerobic glycolysis and OXPHOS to meet their energetic demands such as cardiac or skeletal myocytes, mitochondria play a key role in endothelial function through its ability to generate mtROS involved in endothelial cell signaling and calcium homeostasis [57]. H_2O_2 derived from endothelial mitochondrial NOX4 is an endothelium-derived hyperpolarizing (EDH) factor involved along with NO in the vasodilatation of kidney preglomerular arteries [42], which is supported in the present study by the inhibitory effect of the mitochondrial antioxidant mitoTempo on the endothelial relaxations of control arteries. Reduction of mitochondrial vasodilator H_2O_2 levels in kidney tissues of HFD rats thus contributes to endothelial dysfunction and further emphasizes redox imbalance in kidney vasculature in diet-induced obesity.

The analysis of crucial markers linked to mitochondrial biogenesis and redox metabolism revealed differential expression of NOX4, PGC-1α and MnSOD in the kidney of HFD rats compared to the STD controls. The transcriptional coactivator PGC-1α links mitochondrial biogenesis to the regulation of mitochondrial antioxidant systems and ROS signaling and has been ascribed a protective role in atherogenesis, as it increases expression of antioxidant enzymes in endothelial cells, thus improving NO bioavailability and preventing hyperglycemia-induced mitochondrial dysfunction [50]. In the present study, we demonstrate reduced PGC-1α protein levels in both kidney preglomerular arteries and cortical tissue samples that include glomerular endothelium from HFD-induced obese rats, consistent with the dysregulation of PGC-1α reported in

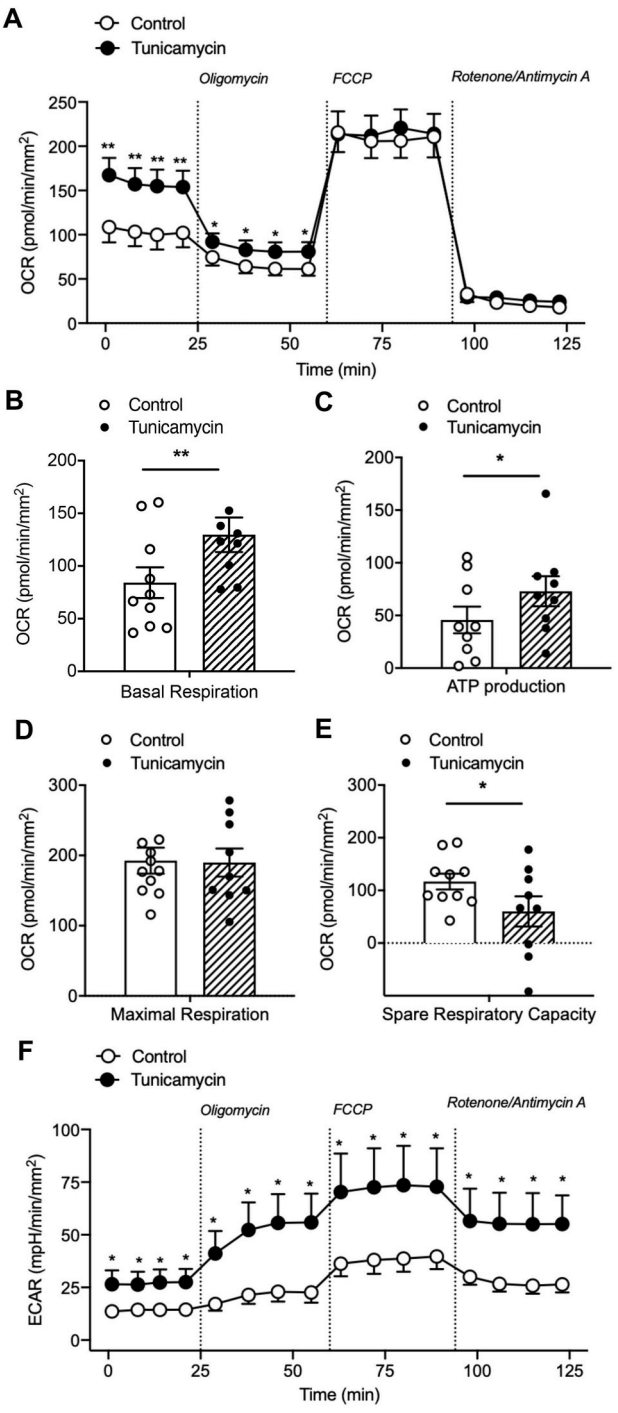

Fig. 10. ER stress enhances mitochondrial respiration in kidney preglomerular arteries (A–C) The *MitoStress test* was performed in freshly isolated preglomerular artery segments using Seahorse technology to measure the oxygen consumption rate (OCR) and extracellular acidification rate (ECAR) in control and tunicamycin treated rats. Sequential injections of oligomycin, FCCP, and rotenone/antimycin A were administered to assess mitochondrial function (A). Renal arteries from ERS rats exhibited increased basal respiration, oxygen consumed for ATP production (A and B), unchanged maximal respiration (A and D), reduced spare respiratory capacity (A and E) and increased ECAR (G) glycolytic activity, compared to controls. Results are expressed as pmol O_2/min (OCR) or mpH/min (ECAR) values and referred to the arterial segment surface in mm^2. Data are shown as means ± SEM of 10–12 control and 10 tunicamycin treated arteries from n = 9 rats from each group. Significant differences between means were analyzed by using unpaired *t*-test. *P < 0.05, **P < 0.01 versus tunicamycin-induced ERs stress rats.

obese patients and animals [58–60], and with the lower gene expression of PGC-1α associated to impaired biogenesis and reduced mitochondrial complex activity reported for the kidney of type 2 diabetic patients with CKD [21]. In the diabetic kidney, reduced gene expression and protein levels of PGC-1α were associated with reduced AMPK activity and lower mtROS levels [21], as shown here in HFD preglomerular arteries and consistent with earlier findings in kidney arteries from obese rodents wherein AMPK activity was also blunted [10]. In the present study, downregulation of PGC-1α was linked to reduced arterial levels of vasodilator H_2O_2 despite unchanged expression of the mitochondrial MnSOD, which contributed to renal endothelial dysfunction in HFD-induced obese rats.

Interestingly, we further demonstrate here that the lower levels of arterial H_2O_2 were linked to reduced expression of NOX4 in preglomerular arteries from diet-induced obese rats, confirming previous data in genetically obese rats wherein down-regulation of NOX4 blunts NOX4-mediated endothelium-dependent relaxations [9]. In contrast to that found in preglomerular arteries, tubule-interstitial injury, fibrosis, and inflammation were associated with upregulation of NOX4 and increased H_2O_2 levels in renal proximal tubule from HFD mice [23], thus suggesting differential pathogenic pathways in kidney vascular and tubular tissues that contribute to renal injury in obesity. NOX4 is a mitochondrial enzyme that directly generates H_2O_2 [61] and is released from endothelial cells by flow-induced shear stress [62]. NOX4 has protective vascular effects by reducing blood pressure [63], inhibiting inflammation and remodeling [64] and promoting angiogenesis via eNOS activation [65]. Furthermore, NOX4-derived H_2O_2 has recently been shown to induce mitochondrial biogenesis and to increase respiratory capacity of skeletal muscle to avoid the deleterious effects of ROS after exercise [60]. In contrast, NOX4 deletion or obesity-induced NOX4 reduction led to decreased expression of genes involved in the control of mitochondrial biogenesis such as *Pgc1α* and *Nrf2* thus reducing levels of PGC-1α and OXPHOS protein complexes [60]. Our findings therefore suggest that obesity-induced decreased expression of endothelial NOX4 and lower H_2O_2 levels in kidney preglomerular arteries not only blunt NOX4-mediated endothelium vasodilatation but also may underlie down-regulation of PGC-1α leading to altered vascular mitochondrial biogenesis and impaired redox balance, thus contributing to the loss of NOX4 protective effects on kidney vasculature [9,42].

Mitochondrial dysregulation involved in the vascular complications of metabolic disorders is produced by alterations in mitochondrial biogenesis and OXPHOS leading to altered mtROS production, cellular apoptosis, and tissue injury [33,35,56]. We demonstrate here that obesity impacts OXPHOS by enhancing mitochondrial bioenergetics and greatly increasing basal and maximal respiration, oxygen consumed for ATP synthesis, proton leak and glycolytic activity of intact kidney preglomerular arteries. Increased mitochondrial activity and electron flow through the ETC may be responsible for the increased mtROS production found in preglomerular arteries from HFD rats. Furthermore, increased proton leak, that is usually higher in vascular myocytes compared to skeletal muscle or cardiac myocytes, is typically associated with increased mtROS production that activates mechanisms promoting proton leak in a protective feed-back loop to reduce ROS and limit damage to the mitochondria [66,67]. Interestingly, the enhanced bioenergetic profile found in kidney arteries from obese rats contrasts with reports on the impact of obesity on bioenergetics of heart and other vascular beds showing augmented mtROS and endothelial dysfunction associated to reduced mitochondrial respiration and lower proton leak in brain [37] and systemic penile arteries [44]. Moreover, reduced respiratory capacity of cardiac myocytes linked to impaired coronary metabolic dilatation has also been reported in rodent models of genetic and diet-induced obesity [36,68]. Interestingly, the higher oxygen consumed for ATP synthesis and maximal respiration of preglomerular arteries from obese rats was associated with the increased relative expression of the cytochrome C oxidase- COX-IV, complex of the ETC suggested to preserve efficiency of respiration under conditions of

limited oxygen bioavailability, and lead adaptative responses to hypoxia [69].

On the other hand, our findings showing enhanced mitochondrial bioenergetics in kidney preglomerular arteries in response to HFD would align with the increased estimated GFR indicative of glomerular hyperfiltration along with the kidney structural abnormalities including glomerular hypertrophy and reduced number of glomeruli demonstrated in the histopathological study of the kidney from HFD-induced obese rats. These changes suggest a metabolic adaptation of kidney preglomerular arteries to the hemodynamic changes aimed to increase intraglomerular pressure and glomerular filtration, therefore increasing metabolic demand in the first stages of obesity-associated kidney disease [70]. In fact, glomerular hyperfiltration is considered a hallmark of renal dysfunction in diabetes and obesity indicative of an unfavorable hemodynamic profile that increases filtration fraction to supply function of injured glomeruli, but later leading to injury of the glomerular filtration barrier, glomerular and podocyte hypertrophy and apoptosis, which accelerates the progression of CKD [7,47], as demonstrated here by the increased protein excretion and reduced urine output indicative of oliguria, along with glomerulomegalia, fibrosis and loss of glomeruli in the HFD-fed rat kidney. While increased respiration has also been reported in isolated mitochondria from whole kidney in HFD-fed mice [23], we first report here a specific bioenergetic adaptative mechanism of kidney preglomerular arteries to lipid overload that increases mitochondrial respiration in contrast to the reduced respiratory capacity induced by obesity in arteries from other vascular beds [36,37,44,68], but likely related to the increased renal blood flow and glomerular hyperfiltration developed to compensate dysfunction of injured glomeruli in obesity-associated kidney disease [7].

Obesity impairs the protein-folding machinery within the ER and activates the ER stress response induced by accumulation of misfolded proteins leading to UPR to maintain ER homeostasis. Chronic activation of ER stress and disruption of UPR contributes to insulin resistance, impaired lipid metabolism and CVD [26,32,71], and has been involved in the pathogenesis of proteinuric kidney disease and diabetic nephropathy [28,29]. The present results demonstrate that HFD induced-obesity activates the UPR pathway in kidney as shown by the increased expression/activity of some ER stress markers such as the chaperone BiP and the three sensors of the UPR pathway in the ER lumen, PERK, ATF6 and IRE1, without significant changes of the ER stress-activated pro-apoptotic factor CHOP. While experimentally-induced ER stress contributes to renal tubular cell and podocyte injury, cellular apoptosis, and renal damage with albuminuria [29,72], we demonstrate here that ER stress impacts kidney arterial function by impairing vasoconstriction and mimicking endothelial dysfunction, redox imbalance and enhanced mitochondrial bioenergetics in renal preglomerular arteries, which suggests that ER stress-induced renal vascular dysfunction contributes to obesity-associated nephropathy.

Reduced α_1-adrenergic vasoconstriction of kidney arteries in tunicamycin-treated rats would be consistent with impairment of the sarco/endoplasmic reticulum calcium ATP_{ase} (SERCA) activity. SERCA regulates cellular calcium homeostasis and maintains ER calcium stores; impairment of the ER fatty acid and lipid composition results in the inhibition of SERCA activity and ER stress, while SERCA overexpression *in vivo* ameliorates chronic ER stress and improves glucose homeostasis [73]. Since the α_1-adrenoceptor in VSM is coupled to the PLC-IP_3-sarcoplasmic reticulum (SR) intracellular calcium release pathway, blunted adrenergic vasoconstriction of kidney arteries from rats with chemically-induced ER stress could be ascribed to the ER stress-induced impairment of the SR calcium store. We have earlier demonstrated that obesity causes SR Ca^{2+} store dysfunction and reduces SR intracellular calcium stores in arterial smooth muscle of coronary and peripheral resistance arteries [74,75], which aligns with the present findings in kidney preglomerular arteries showing reduced adrenergic vasoconstriction under ER conditions.

Interactions between mitochondria and ER have been involved in mitochondrial oxidative stress leading to endothelial dysfunction and to the vascular complications of metabolic disorders [32,33]. ER stress induction in preglomerular arteries impaired endothelium-dependent relaxations mediated by NO as depicted by the lack of inhibitory effect of NOS blockade in ER stress arteries compared to controls, and in agreement with the decreased eNOS promoter activity, blunted eNOS activation and expression and lower NO levels in coronary endothelial cells [32], and the reduced endothelial NOS phosphorylation and impaired endothelium-dependent relaxations in arteries from mice with ER stress induced by hypertension [71]. Whereas tunicamycin-induced oxidative stress via upregulation of endothelial NOX2 and NOX4 and increased NADPH oxidase activity was involved in endothelial dysfunction of aorta and systemic resistance arteries [32], in kidney preglomerular arteries from tunicamycin-treated rats NADPH oxidase activity was unchanged and the non-selective NOX inhibitor apocynin hardly improved endothelial dysfunction. However, a distinctive feature of NOX activity induced by ER stress in kidney preglomerular arteries was the decreased NOX4 expression and reduced vasodilator mitochondrial H_2O_2 levels, which along with the loss of the inhibitory effect of mitoTempo on the endothelium-dependent relaxations suggests that redox imbalance and loss of mitochondrial NOX4-derived vasodilator H_2O_2 contribute to the ER stress-induced endothelial dysfunction similarly to that also found in kidney arteries from HFD obese rats.

Concerning mitochondrial bioenergetics, we demonstrate here that likewise obesity, ER stress enhances basal respiration, oxygen consumed for ATP synthesis and glycolytic activity in renal preglomerular arteries, but reduces spare respiratory capacity in contrast to that reported in cardiac myocytes wherein ER stress inhibited mitochondrial respiration and blunted mitochondrial biogenesis pathways [76]. However, a metabolic adaptative response has been reported in the earlier phases of ER stress by which new ER-mitochondria networks re-organization and increased Ca^{2+} transferred from ER to mitochondria lead to a compensatory enhancement of mitochondrial bioenergetics with increased respiration and higher levels of ATP demanded for the augmented chaperone activity [77]. Furthermore, enhanced mitochondrial respiration associated to improved efficiency of the ETC in response to ER stress has been shown to inhibit ROS accumulation and promote cell survival in eukaryotic cells [78], in agreement with the present results showing increased bioenergetics along with decreased levels of mitochondrial ROS in preglomerular arteries from tunicamycin-induced ER stress rats.

In conclusion, the present findings demonstrate that mitochondrial dysfunction and ER stress underlie renal vascular dysfunction contributing to obesity-associated kidney disease. Decreased mitochondrial biogenesis induced by obesity and ER stress causes redox imbalance with downregulation of NOX4 and PGC1α, reduced vasodilator H_2O_2 levels and endothelial dysfunction. A specific bioenergetic adaptative mechanism that increases respiration and ATP synthesis is developed in preglomerular arteries to reduce mitochondrial oxidative stress and to sustain hemodynamic changes that compensate dysfunction of injured glomeruli in obesity-associated kidney disease. These findings suggest that mitochondria emerge as new therapeutic strategies targets for the vascular complications of obesity-associated nephropathy.

CRediT authorship contribution statement

Cristina Contreras: Writing – review & editing, Visualization, Validation, Supervision, Investigation, Funding acquisition, Formal analysis, Conceptualization. **Mercedes Muñoz:** Methodology, Investigation. **Óscar Freire-Agulleiro:** Methodology, Investigation. **Ánxela Estévez:** Methodology, Investigation. **María Pilar Martínez:** Methodology, Investigation. **Lucia Olmos:** Methodology, Investigation. **Alfonso Gómez del Val:** Methodology, Conceptualization. **Claudia Rodríguez:** Investigation. **Ramona A. Silvestre:** Methodology, Investigation. **Ana Sánchez:** Methodology, Investigation. **Sara Benedito:**

Visualization, Investigation. **Luis Rivera:** Visualization, Validation, Investigation. **Javier Sáenz-Medina:** Validation, Investigation. **Miguel López:** Visualization, Validation, Funding acquisition. **María Elvira López-Oliva:** Visualization, Validation, Methodology, Investigation, Formal analysis. **Dolores Prieto:** Writing – review & editing, Writing – original draft, Validation, Supervision, Formal analysis, Data curation, Conceptualization.

Data and materials Availability

All data are available in the main text or the supplementary materials.

Declaration of competing interest

All the authors declare no conflicts of interest.

Acknowledgments

This research was supported by Grants PID2019-105689RB-I00, PID2022-140536OB-I00 and PID2021-128145NB-I00 from the Spanish Ministry of Science, Innovation, and Universities. We thank Manuel Perales and Francisco Puente for expert technical assistance.

Appendix A. Supplementary data

Supplementary data to this article can be found online at https://doi.org/10.1016/j.redox.2025.103760.

Data availability

Data will be made available on request.

References

[1] H.E. Bays, Adiposopathy is "sick fat" a cardiovascular disease? J. Am. Coll. Cardiol. 57 (2011) 2461–2473, https://doi.org/10.1016/j.jacc.2011.02.038.
[2] F. Rubino, D.E. Cummings, R.H. Eckel, R.V. Cohen, J.P.H. Wilding, W.A. Brown, F. C. Stanford, R.L. Batterham, I.S. Farooqi, N.J. Farpour-Lambert, C.W. le Roux, N. Sattar, L.A. Baur, K.M. Morrison, A. Misra, T. Kadowaki, K.W. Tham, P. Sumithran, W.T. Garvey, J.P. Kirwan, J.M. Fernandez-Real, B.E. Corkey, H. Toplak, A. Kokkinos, R.F. Kushner, F. Branca, J. Valabhji, M. Bluher, S. R. Bornstein, H.J. Grill, E. Ravussin, E. Gregg, N.B. Al Busaidi, N.F. Alfaris, E. Al Ozairi, L.M.S. Carlsson, K. Clement, J.P. Despres, J.B. Dixon, G. Galea, L.M. Kaplan, B. Laferrere, M. Laville, S. Lim, J.R. Luna Fuentes, V.M. Mooney, J. Nadglowski Jr., A. Urudinachi, M. Olszanecka-Glinianowicz, A. Pan, F. Pattou, P.R. Schauer, M. H. Tschop, M.T. van der Merwe, R. Vettor, G. Mingrone, Definition and diagnostic criteria of clinical obesity, Lancet Diabetes Endocrinol. 13 (2025) 221–262, https://doi.org/10.1016/S2213-8587(24)00316-4.
[3] C.K. Abrass, Cellular lipid metabolism and the role of lipids in progressive renal disease, Am. J. Nephrol. 24 (2004) 46–53, https://doi.org/10.1159/000075925.
[4] H. Kramer, A. Luke, A. Bidani, G. Cao, R. Cooper, D. McGee, Obesity and prevalent and incident CKD: the Hypertension Detection and Follow-Up Program, Am. J. Kidney Dis. 46 (2005) 587–594, https://doi.org/10.1053/j.ajkd.2005.06.007.
[5] M.C. Foster, S.J. Hwang, M.G. Larson, J.H. Lichtman, N.I. Parikh, R.S. Vasan, D. Levy, C.S. Fox, Overweight, obesity, and the development of stage 3 CKD: the Framingham Heart Study, Am. J. Kidney Dis. 52 (2008) 39–48, https://doi.org/10.1053/j.ajkd.2008.03.003.
[6] A.P. de Vries, P. Ruggenenti, X.Z. Ruan, M. Praga, J.M. Cruzado, I.M. Bajema, V. D. D'Agati, H.J. Lamb, D. Pongrac Barlovic, R. Hojs, M. Abbate, R. Rodriquez, C. E. Mogensen, E. Porrini, E.-E.W.G. Diabesity, Fatty kidney: emerging role of ectopic lipid in obesity-related renal disease, Lancet Diabetes Endocrinol. 2 (2014) 417–426, https://doi.org/10.1016/S2213-8587(14)70065-8.
[7] A.J. Kwakernaak, T.J. Toering, G. Navis, Body mass index and body fat distribution as renal risk factors: a focus on the role of renal haemodynamics, Nephrol. Dial. Transplant. 28 (Suppl 4) (2013) iv42–iv49, https://doi.org/10.1093/ndt/gft331.
[8] K. Sharma, Obesity, oxidative stress, and fibrosis in chronic kidney disease, Kidney Int. Suppl. (4) (2011) 113–117, https://doi.org/10.1038/kisup.2014.21, 2014.
[9] M. Munoz, M.E. Lopez-Oliva, C. Rodriguez, M.P. Martinez, J. Saenz-Medina, A. Sanchez, B. Climent, S. Benedito, A. Garcia-Sacristan, L. Rivera, M. Hernandez, D. Prieto, Differential contribution of Nox1, Nox2 and Nox4 to kidney vascular oxidative stress and endothelial dysfunction in obesity, Redox Biol. 28 (2020) 101330, https://doi.org/10.1016/j.redox.2019.101330.
[10] C. Rodríguez, A. Sánchez, J. Sáenz-Medina, M. Muñoz, M. Hernández, M. López, L. Rivera, C. Contreras, D. Prieto, Activation of AMP kinase ameliorates kidney vascular dysfunction, oxidative stress and inflammation in rodent models of obesity, Br. J. Pharmacol. 178 (2021) 4085–4103, https://doi.org/10.1111/bph.15600.
[11] M. Forte, S. Palmerio, F. Bianchi, M. Volpe, S. Rubattu, Mitochondrial complex I deficiency and cardiovascular diseases: current evidence and future directions, J. Mol. Med. (Berl.) 97 (2019) 579–591, https://doi.org/10.1007/s00109-019-01771-3.
[12] M. Herman-Edelstein, P. Scherzer, A. Tobar, M. Levi, U. Gafter, Altered renal lipid metabolism and renal lipid accumulation in human diabetic nephropathy, J. Lipid Res. 55 (2014) 561–572, https://doi.org/10.1194/jlr.P040501.
[13] A. Diaz-Vegas, P. Sanchez-Aguilera, J.R. Krycer, P.E. Morales, M. Monsalves-Alvarez, M. Cifuentes, B.A. Rothermel, S. Lavandero, Is mitochondrial dysfunction a common root of noncommunicable chronic diseases? Endocr. Rev. 41 (2020) https://doi.org/10.1210/endrev/bnaa005.
[14] D.L. Kirkman, A.T. Robinson, M.J. Rossman, D.R. Seals, D.G. Edwards, Mitochondrial contributions to vascular endothelial dysfunction, arterial stiffness, and cardiovascular diseases, Am. J. Physiol. Heart Circ. Physiol. 320 (2021) H2080–H2100, https://doi.org/10.1152/ajpheart.00917.2020.
[15] Y. Han, X. Xu, C. Tang, P. Gao, X. Chen, X. Xiong, M. Yang, S. Yang, X. Zhu, S. Yuan, F. Liu, L. Xiao, Y.S. Kanwar, L. Sun, Reactive oxygen species promote tubular injury in diabetic nephropathy: the role of the mitochondrial ros-txnip-nlrp3 biological axis, Redox Biol. 16 (2018) 32–46, https://doi.org/10.1016/j.redox.2018.02.013.
[16] M. Sedeek, G. Callera, A. Montezano, A. Gutsol, F. Heitz, C. Szyndralewiez, P. Page, C.R. Kennedy, K.D. Burns, R.M. Touyz, R.L. Hebert, Critical role of Nox4-based NADPH oxidase in glucose-induced oxidative stress in the kidney: implications in type 2 diabetic nephropathy, Am. J. Physiol. Ren. Physiol. 299 (2010) F1348–F1358, https://doi.org/10.1152/ajprenal.00028.2010.
[17] J.C. Jha, S.P. Gray, D. Barit, J. Okabe, A. El-Osta, T. Namikoshi, V. Thallas-Bonke, K. Wingler, C. Szyndralewiez, F. Heitz, R.M. Touyz, M.E. Cooper, H.H. Schmidt, K. A. Jandeleit-Dahm, Genetic targeting or pharmacologic inhibition of NADPH oxidase nox4 provides renoprotection in long-term diabetic nephropathy, J. Am. Soc. Nephrol. 25 (2014) 1237–1254, https://doi.org/10.1681/ASN.2013070810.
[18] J.C. Jha, V. Thallas-Bonke, C. Banal, S.P. Gray, B.S. Chow, G. Ramm, S.E. Quaggin, M.E. Cooper, H.H. Schmidt, K.A. Jandeleit-Dahm, Podocyte-specific Nox4 deletion affords renoprotection in a mouse model of diabetic nephropathy, Diabetologia 59 (2016) 379–389, https://doi.org/10.1007/s00125-015-3796-0.
[19] A.E. Decleves, A.V. Mathew, R. Cunard, K. Sharma, AMPK mediates the initiation of kidney disease induced by a high-fat diet, J. Am. Soc. Nephrol. 22 (2011) 1846–1855, https://doi.org/10.1681/ASN.2011010026.
[20] T. Nishikawa, D. Edelstein, X.L. Du, S. Yamagishi, T. Matsumura, Y. Kaneda, M. A. Yorek, D. Beebe, P.J. Oates, H.P. Hammes, I. Giardino, M. Brownlee, Normalizing mitochondrial superoxide production blocks three pathways of hyperglycaemic damage, Nature 404 (2000) 787–790, https://doi.org/10.1038/35008121.
[21] L.L. Dugan, Y.H. You, S.S. Ali, M. Diamond-Stanic, S. Miyamoto, A.E. DeCleves, A. Andreyev, T. Quach, S. Ly, G. Shekhtman, W. Nguyen, A. Chepetan, T.P. Le, L. Wang, M. Xu, K.P. Paik, A. Fogo, B. Viollet, A. Murphy, F. Brosius, R.K. Naviaux, K. Sharma, AMPK dysregulation promotes diabetes-related reduction of superoxide and mitochondrial function, J. Clin. Investig. 123 (2013) 4888–4899, https://doi.org/10.1172/JCI66218.
[22] K. Sharma, Obesity and diabetic kidney disease: role of oxidant stress and redox balance, Antioxidants Redox Signal. 25 (2016) 208–216, https://doi.org/10.1089/ars.2016.6696.
[23] C. Ruggiero, M. Ehrenshaft, E. Cleland, K. Stadler, High-fat diet induces an initial adaptation of mitochondrial bioenergetics in the kidney despite evident oxidative stress and mitochondrial ROS production, Am. J. Physiol. Endocrinol. Metab. 300 (2011) E1047–E1058, https://doi.org/10.1152/ajpendo.00666.2010.
[24] S. Munusamy, J.M. do Carmo, J.P. Hosler, J.E. Hall, Obesity-induced changes in kidney mitochondria and endoplasmic reticulum in the presence or absence of leptin, Am. J. Physiol. Ren. Physiol. 309 (2015) F731–F743, https://doi.org/10.1152/ajprenal.00188.2015.
[25] C. Hetz, K. Zhang, R.J. Kaufman, Mechanisms, regulation and functions of the unfolded protein response, Nat. Rev. Mol. Cell Biol. 21 (2020) 421–438, https://doi.org/10.1038/s41580-020-0250-z.
[26] U. Ozcan, Q. Cao, E. Yilmaz, A.H. Lee, N.N. Iwakoshi, E. Ozdelen, G. Tuncman, C. Gorgun, L.H. Glimcher, G.S. Hotamisligil, Endoplasmic reticulum stress links obesity, insulin action, and type 2 diabetes, Science 306 (2004) 457–461, https://doi.org/10.1126/science.1103160.
[27] G.S. Hotamisligil, Inflammation and endoplasmic reticulum stress in obesity and diabetes, Int. J. Obes. 32 (Suppl 7) (2008) S52–S54, https://doi.org/10.1038/ijo.2008.238.
[28] A.V. Cybulsky, Endoplasmic reticulum stress, the unfolded protein response and autophagy in kidney diseases, Nat. Rev. Nephrol. 13 (2017) 681–696, https://doi.org/10.1038/nrneph.2017.129.
[29] R. Inagi, Y. Ishimoto, M. Nangaku, Proteostasis in endoplasmic reticulum–new mechanisms in kidney disease, Nat. Rev. Nephrol. 10 (2014) 369–378, https://doi.org/10.1038/nrneph.2014.67.
[30] A. Zhuang, J.M. Forbes, Stress in the kidney is the road to pERdition: is endoplasmic reticulum stress a pathogenic mediator of diabetic nephropathy? J. Endocrinol. 222 (2014) R97–R111, https://doi.org/10.1530/JOE-13-0517.
[31] A. Amin, S.K. Choi, M. Galan, M. Kassan, M. Partyka, P. Kadowitz, D. Henrion, M. Trebak, S. Belmadani, K. Matrougui, Chronic inhibition of endoplasmic reticulum stress and inflammation prevents ischaemia-induced vascular pathology in type II diabetic mice, J. Pathol. 227 (2012) 165–174, https://doi.org/10.1002/path.3960.

[32] M. Galan, M. Kassan, P.J. Kadowitz, M. Trebak, S. Belmadani, K. Matrougui, Mechanism of endoplasmic reticulum stress-induced vascular endothelial dysfunction, Biochim. Biophys. Acta 1843 (2014) 1063–1075, https://doi.org/10.1016/j.bbamcr.2014.02.009.
[33] Z. Safiedeen, R. Andriantsitohaina, M.C. Martinez, Dialogue between endoplasmic reticulum and mitochondria as a key actor of vascular dysfunction associated to metabolic disorders, Int. J. Biochem. Cell Biol. 77 (2016) 10–14, https://doi.org/10.1016/j.biocel.2016.05.011.
[34] H.H. Szeto, S. Liu, Y. Soong, N. Alam, G.T. Prusky, S.V. Seshan, Protection of mitochondria prevents high-fat diet-induced glomerulopathy and proximal tubular injury, Kidney Int. 90 (2016) 997–1011, https://doi.org/10.1016/j.kint.2016.06.013.
[35] T.J. Kizhakekuttu, J. Wang, K. Dharmashankar, R. Ying, D.D. Gutterman, J.A. Vita, M.E. Widlansky, Adverse alterations in mitochondrial function contribute to type 2 diabetes mellitus-related endothelial dysfunction in humans, Arterioscler. Thromb. Vasc. Biol. 32 (2012) 2531–2539, https://doi.org/10.1161/ATVBAHA.112.256024.
[36] G. Guarini, T. Kiyooka, V. Ohanyan, Y.F. Pung, M. Marzilli, Y.R. Chen, C.L. Chen, P. T. Kang, J.P. Hardwick, C.L. Kolz, L. Yin, G.L. Wilson, I. Shokolenko, J. G. Dobson Jr., R. Fenton, W.M. Chilian, Impaired coronary metabolic dilation in the metabolic syndrome is linked to mitochondrial dysfunction and mitochondrial DNA damage, Basic Res. Cardiol. 111 (2016) 29, https://doi.org/10.1007/s00395-016-0547-4.
[37] I. Merdzo, I. Rutkai, V.N. Sure, C.A. McNulty, P.V. Katakam, D.W. Busija, Impaired mitochondrial respiration in large cerebral arteries of rats with type 2 diabetes, J. Vasc. Res. 54 (2017) 1–12, https://doi.org/10.1159/000454812.
[38] S. Herget-Rosenthal, G. Marggraf, J. Husing, F. Goring, F. Pietruck, O. Janssen, T. Philipp, A. Kribben, Early detection of acute renal failure by serum cystatin C, Kidney Int. 66 (2004) 1115–1122, https://doi.org/10.1111/j.1523-1755.2004.00861.x.
[39] S. Song, M. Meyer, T.R. Turk, B. Wilde, T. Feldkamp, R. Assert, K. Wu, A. Kribben, O. Witzke, Serum cystatin C in mouse models: a reliable and precise marker for renal function and superior to serum creatinine, Nephrol. Dial. Transplant. 24 (2009) 1157–1161, https://doi.org/10.1093/ndt/gfn626.
[40] G.K. Rangan, G.H. Tesch, Quantification of renal pathology by image analysis, Nephrology 12 (2007) 553–558, https://doi.org/10.1111/j.1440-1797.2007.00855.x.
[41] M. Munoz, M.E. Lopez-Oliva, E. Pinilla, M.P. Martinez, A. Sanchez, C. Rodriguez, A. Garcia-Sacristan, M. Hernandez, L. Rivera, D. Prieto, CYP epoxygenase-derived H(2)O(2) is involved in the endothelium-derived hyperpolarization (EDH) and relaxation of intrarenal arteries, Free Radic. Biol. Med. 106 (2017) 168–183, https://doi.org/10.1016/j.freeradbiomed.2017.02.031.
[42] M. Munoz, M.P. Martinez, M.E. Lopez-Oliva, C. Rodriguez, C. Corbacho, J. Carballido, A. Garcia-Sacristan, M. Hernandez, L. Rivera, J. Saenz-Medina, D. Prieto, Hydrogen peroxide derived from NADPH oxidase 4- and 2 contributes to the endothelium-dependent vasodilatation of intrarenal arteries, Redox Biol. 19 (2018) 92–104, https://doi.org/10.1016/j.redox.2018.08.004.
[43] A. Gomez Del Val, C. Contreras, M. Munoz, J. Saenz-Medina, M. Mohamed, L. Rivera, A. Sanchez, D. Prieto, Activation of mitoK(ATP) channels induces penile vasodilation and inhibits mitochondrial respiration and ROS production: role of NO, Free Radic. Biol. Med. 217 (2024) 15–28, https://doi.org/10.1016/j.freeradbiomed.2024.03.007.
[44] A. Gomez Del Val, A. Sanchez, O. Freire-Agulleiro, M.P. Martinez, M. Munoz, L. Olmos, J.S. Medina, S.G. Comerma-Steffensen, U. Simonsen, L. Rivera, M. Lopez, C. Contreras, D. Prieto, Penile endothelial dysfunction, impaired redox metabolism and blunted mitochondrial bioenergetics in diet-induced obesity: compensatory role of H(2)O(2), Free Radic. Biol. Med. 230 (2025) 222–233, https://doi.org/10.1016/j.freeradbiomed.2025.02.004.
[45] E. Jebelovszki, C. Kiraly, N. Erdei, A. Feher, E.T. Pasztor, I. Rutkai, T. Forster, I. Edes, A. Koller, Z. Bagi, High-fat diet-induced obesity leads to increased NO sensitivity of rat coronary arterioles: role of soluble guanylate cyclase activation, Am. J. Physiol. Heart Circ. Physiol. 294 (2008) H2558–H2564, https://doi.org/10.1152/ajpheart.01198.2007.
[46] R. Hojs, S. Bevc, R. Ekart, M. Gorenjak, L. Puklavec, Serum cystatin C as an endogenous marker of renal function in patients with mild to moderate impairment of kidney function, Nephrol. Dial. Transplant. 21 (2006) 1855–1862, https://doi.org/10.1093/ndt/gfl073.
[47] A. Chagnac, B. Zingerman, B. Rozen-Zvi, M. Herman-Edelstein, Consequences of glomerular hyperfiltration: the role of physical forces in the pathogenesis of chronic kidney disease in diabetes and obesity, Nephron 143 (2019) 38–42, https://doi.org/10.1159/000499486.
[48] D. Prieto, C. Contreras, A. Sanchez, Endothelial dysfunction, obesity and insulin resistance, Curr. Vasc. Pharmacol. 12 (2014) 412–426, https://doi.org/10.2174/15701611126661404232210 08.
[49] M. Muñoz, M. Elvira Lopez-Oliva, E. Pinilla, M. Pilar Martinez, A. Sanchez, C. Rodriguez, A. Garcia-Sacristan, M. Hernandez, L. Rivera, D. Prieto, CYP epoxygenase-derived H2O2 is involved in the endothelium-derived hyperpolarization (EDH) and relaxation of intrarenal arteries, Free Radic. Biol. Med. 106 (2017) 168–183, https://doi.org/10.1016/j.freeradbiomed.2017.02.031.
[50] I. Valle, A. Alvarez-Barrientos, E. Arza, S. Lamas, M. Monsalve, PGC-1alpha regulates the mitochondrial antioxidant defense system in vascular endothelial cells, Cardiovasc. Res. 66 (2005) 562–573, https://doi.org/10.1016/j.cardiores.2005.01.026.
[51] H.O. Steinberg, H. Chaker, R. Leaming, A. Johnson, G. Brechtel, A.D. Baron, Obesity/insulin resistance is associated with endothelial dysfunction. Implications for the syndrome of insulin resistance, J. Clin. Investig. 97 (1996) 2601–2610, https://doi.org/10.1172/JCI118709.
[52] F. Perticone, R. Ceravolo, M. Candigliota, G. Ventura, S. Iacopino, F. Sinopoli, P. L. Mattioli, Obesity and body fat distribution induce endothelial dysfunction by oxidative stress: protective effect of vitamin C, Diabetes 50 (2001) 159–165, https://doi.org/10.2337/diabetes.50.1.159.
[53] A.K. Doughan, D.G. Harrison, S.I. Dikalov, Molecular mechanisms of angiotensin II-mediated mitochondrial dysfunction: linking mitochondrial oxidative damage and vascular endothelial dysfunction, Circ. Res. 102 (2008) 488–496, https://doi.org/10.1161/CIRCRESAHA.107.162800.
[54] R.A. Gioscia-Ryan, T.J. LaRocca, A.L. Sindler, M.C. Zigler, M.P. Murphy, D.R. Seals, Mitochondria-targeted antioxidant (MitoQ) ameliorates age-related arterial endothelial dysfunction in mice, J. Physiol. 592 (2014) 2549–2561, https://doi.org/10.1113/jphysiol.2013.268680.
[55] S.Y. Park, E.J. Pekas, R.J. Headid 3rd, W.M. Son, T.K. Wooden, J. Song, G. Layec, S. K. Yadav, P.K. Mishra, I.I. Pipinos, Acute mitochondrial antioxidant intake improves endothelial function, antioxidant enzyme activity, and exercise tolerance in patients with peripheral artery disease, Am. J. Physiol. Heart Circ. Physiol. 319 (2020) H456–H467, https://doi.org/10.1152/ajpheart.00235.2020.
[56] S.M. Shenouda, M.E. Widlansky, K. Chen, G. Xu, M. Holbrook, C.E. Tabit, N. M. Hamburg, A.A. Frame, T.L. Caiano, M.A. Kluge, M.A. Duess, A. Levit, B. Kim, M. L. Hartman, L. Joseph, O.S. Shirihai, J.A. Vita, Altered mitochondrial dynamics contributes to endothelial dysfunction in diabetes mellitus, Circulation 124 (2011) 444–453, https://doi.org/10.1161/CIRCULATIONAHA.110.014506.
[57] M.E. Widlansky, D.D. Gutterman, Regulation of endothelial function by mitochondrial reactive oxygen species, Antioxidants Redox Signal. 15 (2011) 1517–1530, https://doi.org/10.1089/ars.2010.3642.
[58] C. Wang, L. Li, S. Liu, G. Liao, L. Li, Y. Chen, J. Cheng, Y. Lu, J. Liu, GLP-1 receptor agonist ameliorates obesity-induced chronic kidney injury via restoring renal metabolism homeostasis, PLoS One 13 (2018) e0193473, https://doi.org/10.1371/journal.pone.0193473.
[59] S. Perez, S. Rius-Perez, I. Finamor, P. Marti-Andres, I. Prieto, R. Garcia, M. Monsalve, J. Sastre, Obesity causes PGC-1alpha deficiency in the pancreas leading to marked IL-6 upregulation via NF-kappaB in acute pancreatitis, J. Pathol. 247 (2019) 48–59, https://doi.org/10.1002/path.5166.
[60] C.E. Xirouchaki, Y. Jia, M.J. McGrath, S. Greatorex, M. Tran, T.L. Merry, D. Hong, M.J. Eramo, S.C. Broome, J.S.T. Woodhead, F. D'Souza R, J. Gallagher, E. Salimova, C. Huang, R.B. Schittenhelm, J. Sadoshima, M.J. Watt, C.A. Mitchell, T. Tiganis, Skeletal muscle NOX4 is required for adaptive responses that prevent insulin resistance, Sci. Adv. 7 (2021) eabl4988, https://doi.org/10.1126/sciadv.abl4988.
[61] K.D. Martyn, L.M. Frederick, K. von Loehneysen, M.C. Dinauer, U.G. Knaus, Functional analysis of Nox4 reveals unique characteristics compared to other NADPH oxidases, Cell. Signal. 18 (2006) 69–82, https://doi.org/10.1016/j.cellsig.2005.03.023.
[62] F.J. Sanchez-Gomez, E. Calvo, R. Breton-Romero, M. Fierro-Fernandez, N. Anilkumar, A.M. Shah, K. Schroder, R.P. Brandes, J. Vazquez, S. Lamas, NOX4-dependent Hydrogen peroxide promotes shear stress-induced SHP2 sulfenylation and eNOS activation, Free Radic. Biol. Med. 89 (2015) 419–430, https://doi.org/10.1016/j.freeradbiomed.2015.08.014.
[63] R. Ray, C.E. Murdoch, M. Wang, C.X. Santos, M. Zhang, S. Alom-Ruiz, N. Anilkumar, A. Ouattara, A.C. Cave, S.J. Walker, D.J. Grieve, R.L. Charles, P. Eaton, A.C. Brewer, A.M. Shah, Endothelial Nox4 NADPH oxidase enhances vasodilatation and reduces blood pressure in vivo, Arterioscler. Thromb. Vasc. Biol. 31 (2011) 1368–1376, https://doi.org/10.1161/ATVBAHA.110.219238.
[64] S.P. Gray, E. Di Marco, K. Kennedy, P. Chew, J. Okabe, A. El-Osta, A.C. Calkin, E. A. Biessen, R.M. Touyz, M.E. Cooper, H.H. Schmidt, K.A. Jandeleit-Dahm, Reactive oxygen species can provide atheroprotection via NOX4-Dependent inhibition of inflammation and vascular remodeling, Arterioscler. Thromb. Vasc. Biol. 36 (2016) 295–307, https://doi.org/10.1161/ATVBAHA.115.307012.
[65] S.M. Craige, K. Chen, Y. Pei, C. Li, X. Huang, C. Chen, R. Shibata, K. Sato, K. Walsh, J.F. Keaney Jr., NADPH oxidase 4 promotes endothelial angiogenesis through endothelial nitric oxide synthase activation, Circulation 124 (2011) 731–740, https://doi.org/10.1161/CIRCULATIONAHA.111.030775.
[66] S.Y. Park, J.R. Gifford, R.H. Andtbacka, J.D. Trinity, J.R. Hyngstrom, R.S. Garten, N.A. Diakos, S.J. Ives, F. Dela, S. Larsen, S. Drakos, R.S. Richardson, Cardiac, skeletal, and smooth muscle mitochondrial respiration: are all mitochondria created equal? Am. J. Physiol. Heart Circ. Physiol. 307 (2014) H346–H352, https://doi.org/10.1152/ajpheart.00227.2014.
[67] J. Cheng, G. Nanayakkara, Y. Shao, R. Cueto, L. Wang, W.Y. Yang, Y. Tian, H. Wang, X. Yang, Mitochondrial proton leak plays a critical role in pathogenesis of cardiovascular diseases, Adv. Exp. Med. Biol. 982 (2017) 359–370, https://doi.org/10.1007/978-3-319-55330-6_20.
[68] A.L. Sverdlov, A. Elezaby, J.B. Behring, M.M. Bachschmid, I. Luptak, V.H. Tu, D. A. Siwik, E.J. Miller, M. Liesa, O.S. Shirihai, D.R. Pimentel, R.A. Cohen, W. S. Colucci, High fat, high sucrose diet causes cardiac mitochondrial dysfunction due in part to oxidative post-translational modification of mitochondrial complex II, J. Mol. Cell. Cardiol. 78 (2015) 165–173, https://doi.org/10.1016/j.yjmcc.2014.07.018.
[69] R. Fukuda, H. Zhang, J.W. Kim, L. Shimoda, C.V. Dang, G.L. Semenza, HIF-1 regulates cytochrome oxidase subunits to optimize efficiency of respiration in hypoxic cells, Cell 129 (2007) 111–122, https://doi.org/10.1016/j.cell.2007.01.047.
[70] V.D. D'Agati, A. Chagnac, A.P. de Vries, M. Levi, E. Porrini, M. Herman-Edelstein, M. Praga, Obesity-related glomerulopathy: clinical and pathologic characteristics

and pathogenesis, Nat. Rev. Nephrol. 12 (2016) 453–471, https://doi.org/10.1038/nrneph.2016.75.
[71] M. Kassan, M. Galan, M. Partyka, Z. Saifudeen, D. Henrion, M. Trebak, K. Matrougui, Endoplasmic reticulum stress is involved in cardiac damage and vascular endothelial dysfunction in hypertensive mice, Arterioscler. Thromb. Vasc. Biol. 32 (2012) 1652–1661, https://doi.org/10.1161/ATVBAHA.112.249318.
[72] T. Kawakami, R. Inagi, H. Takano, S. Sato, J.R. Ingelfinger, T. Fujita, M. Nangaku, Endoplasmic reticulum stress induces autophagy in renal proximal tubular cells, Nephrol. Dial. Transplant. 24 (2009) 2665–2672, https://doi.org/10.1093/ndt/gfp215.
[73] S. Fu, L. Yang, P. Li, O. Hofmann, L. Dicker, W. Hide, X. Lin, S.M. Watkins, A. R. Ivanov, G.S. Hotamisligil, Aberrant lipid metabolism disrupts calcium homeostasis causing liver endoplasmic reticulum stress in obesity, Nature 473 (2011) 528–531, https://doi.org/10.1038/nature09968.
[74] B. Climent, E. Santiago, A. Sanchez, M. Munoz-Picos, F. Perez-Vizcaino, A. Garcia-Sacristan, L. Rivera, D. Prieto, Metabolic syndrome inhibits store-operated Ca(2+) entry and calcium-induced calcium-release mechanism in coronary artery smooth muscle, Biochem. Pharmacol. 182 (2020) 114222, https://doi.org/10.1016/j.bcp.2020.114222.
[75] A. Sanchez, C. Contreras, B. Climent, A. Gutierrez, M. Munoz, A. Garcia-Sacristan, M. Lopez, L. Rivera, D. Prieto, Impaired Ca(2+) handling in resistance arteries from genetically obese Zucker rats: role of the PI3K, ERK1/2 and PKC signaling pathways, Biochem. Pharmacol. 152 (2018) 114–128, https://doi.org/10.1016/j.bcp.2018.03.020.
[76] A. Prola, Z. Nichtova, J. Pires Da Silva, J. Piquereau, K. Monceaux, A. Guilbert, M. Gressette, R. Ventura-Clapier, A. Garnier, I. Zahradnik, M. Novotova, C. Lemaire, Endoplasmic reticulum stress induces cardiac dysfunction through architectural modifications and alteration of mitochondrial function in cardiomyocytes, Cardiovasc. Res. 115 (2019) 328–342, https://doi.org/10.1093/cvr/cvy197.
[77] R. Bravo, J.M. Vicencio, V. Parra, R. Troncoso, J.P. Munoz, M. Bui, C. Quiroga, A. E. Rodriguez, H.E. Verdejo, J. Ferreira, M. Iglewski, M. Chiong, T. Simmen, A. Zorzano, J.A. Hill, B.A. Rothermel, G. Szabadkai, S. Lavandero, Increased ER-mitochondrial coupling promotes mitochondrial respiration and bioenergetics during early phases of ER stress, J. Cell Sci. 124 (2011) 2143–2152, https://doi.org/10.1242/jcs.080762.
[78] J. Knupp, P. Arvan, A. Chang, Increased mitochondrial respiration promotes survival from endoplasmic reticulum stress, Cell Death Differ. 26 (2019) 487–501, https://doi.org/10.1038/s41418-018-0133-4.